THERMALLY EFFECTIVE AND EFFICIENT COOLING TECHNOLOGIES FOR ADVANCED GAS TURBINES

UTSR Workshop Virginia Tech

1 November 2016

Forrest Ames, UND

Sumanta Acharya, Illinois Institute of Technology

James Downs, FTT (Advisory)

PRESENTATION OVERVIEW

- Conceptual approach to our project
- Briefly describe the four phases the present program
- Discuss how FEA analysis is used to drive the development of internal cooling methods based on external boundary conditions
- Present recently acquired heat transfer data and discus preparations for film cooling measurements for external heat load evaluation in our low speed cascade test section.
- Internal cooling methods development: Bench scale rig.
- Computational methods: Clarifying physics of film cooling and internal cooling & serving to refine model boundary conditions.
- Warm cascade testing will be used for cooling system evaluation and validation based on comparing the results with an enhanced FEA vane model.

CONCEPTUAL APPROACH

- Component cooling methods need to provide highly effective, efficient, locally prescribed, and reliable cooling systems.
- Ideal internal cooling methods
  - Achieve good levels of internal effectiveness
  - Discharge spent cooling air onto surfaces in optimum films.
- Leading edge regions can be cooled internally:
  - Achieving a high level of overall effectiveness
  - Eliminating the disruption of shower-head films and the potential for clogging
  - Improving downstream film cooling levels.
- The efficiency and effectiveness of downstream cooling levels can be improved by better matching of internal cooling concept with external films (counter cooling).
- Covered trailing edge designs offer the best thermal protection:
  - There is no clear evidence of higher losses compared to pressure side cutbacks.

FOUR PHASE PROGRAM

DETAILED RESEARCH PLAN

Phase 1: FEA Cooling Model Development

1. External heat load prediction (UND)
2. Internal cooling designation (UND)
3. External film and heat transfer b.c. (UND)
4. FDA/FEA development and analysis (UND,FTT)

Phase 2a: Internal cooling tests

UND's bench scale internal heat transfer and flow test rig.

Phase 2b: Internal cooling computations

IIT's computational research group

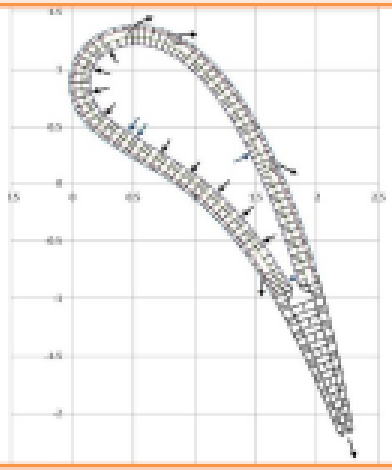

Phase 3a: External film and heat transfer tests

UND's Large Scale Cascade Wind Tunnel

Phase 3b: External heat load computations

IIT's computational research group

Phase 4: Cooling system validation

1. FEA model refinement and predictions (UND)
2. Warm cascade validation testing (IIT)

FINITE DIFFERENCE ANALYSIS

- Finite difference analysis provides a means to match external heat loads with appropriate cooling design and coolant flows.
- Results of analysis suggest regions of overcooling and regions where cooling is more challenging.
- The present objective is to demonstrate the successful integration of three cooling technologies into a cooling design.

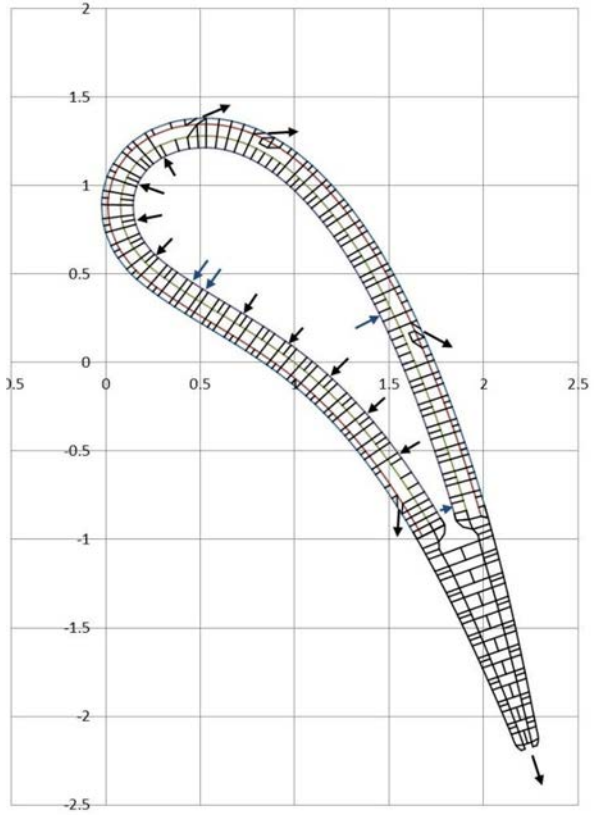

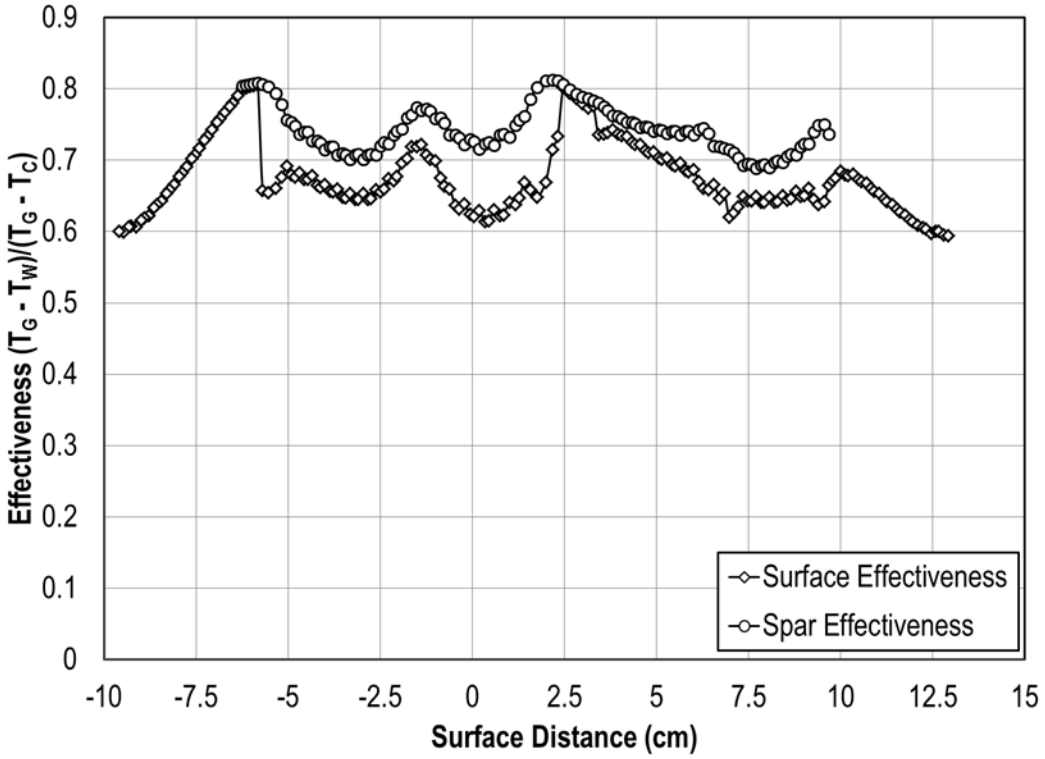

FINITE ELEMENT ANALYSIS ANSYS

The boundary conditions developed for the FDA were imported into a 2D FEA in ANSYS. The FDA and FEA analyses point to areas were cooling levels can be optimized.

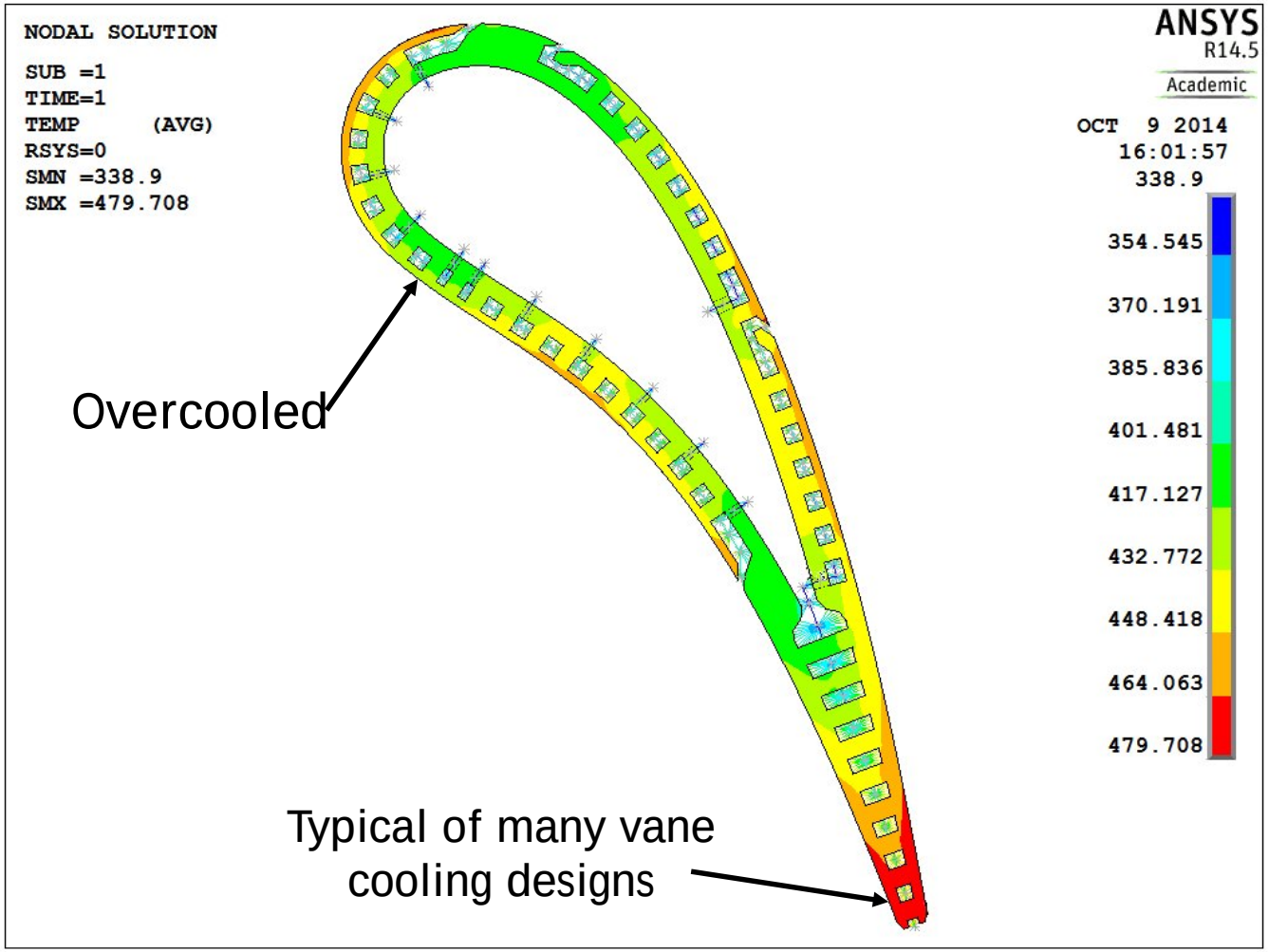

Large Scale Low Speed Cascade Testing

- UND's large scale cascade has been used to evaluate midspan and suction surface heat transfer distributions over a relevant range in turbulence conditions.
- Soon it will be used to evaluate film cooling effectiveness and the influence of film cooling on heat transfer.
- UND/IIT will use these data to help refine the heat transfer boundary condition for the warm cascade test.

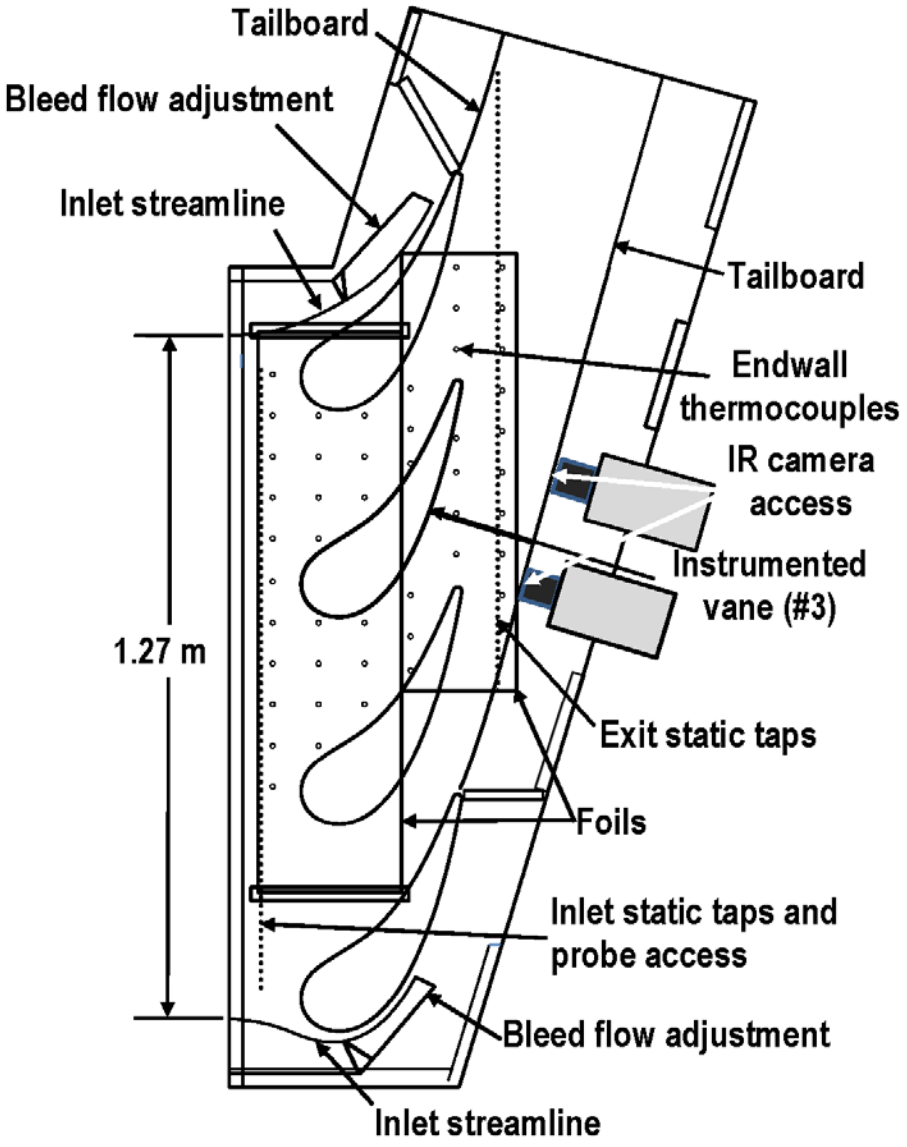

MIDSPAN HEAT TRANSFER DISTRIBUTIONS

- The vane was designed with a large leading edge and an aft loaded pressure distribution. The minimum pressure is at about 70% surface.
- The larger leading edge reduces heat load and the aft loading pushes transition downstream.
- At the 500,000 Reynolds number the pressure surface is largely laminar while the suction surface is largely transitional.
- The six elevated turbulence levels show significant incremental augmentation for levels ranging from 3.5% to 17.4%.

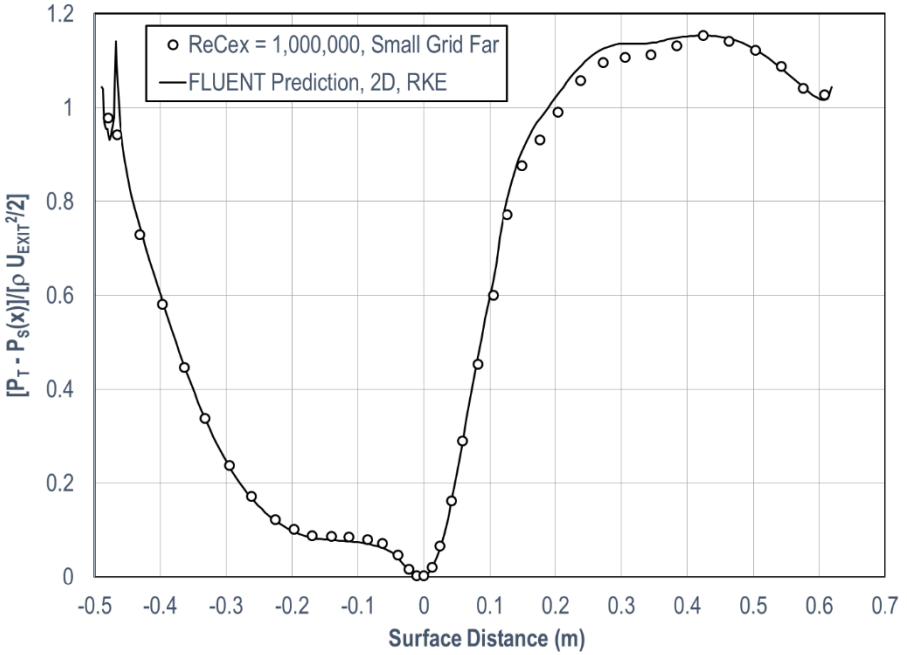

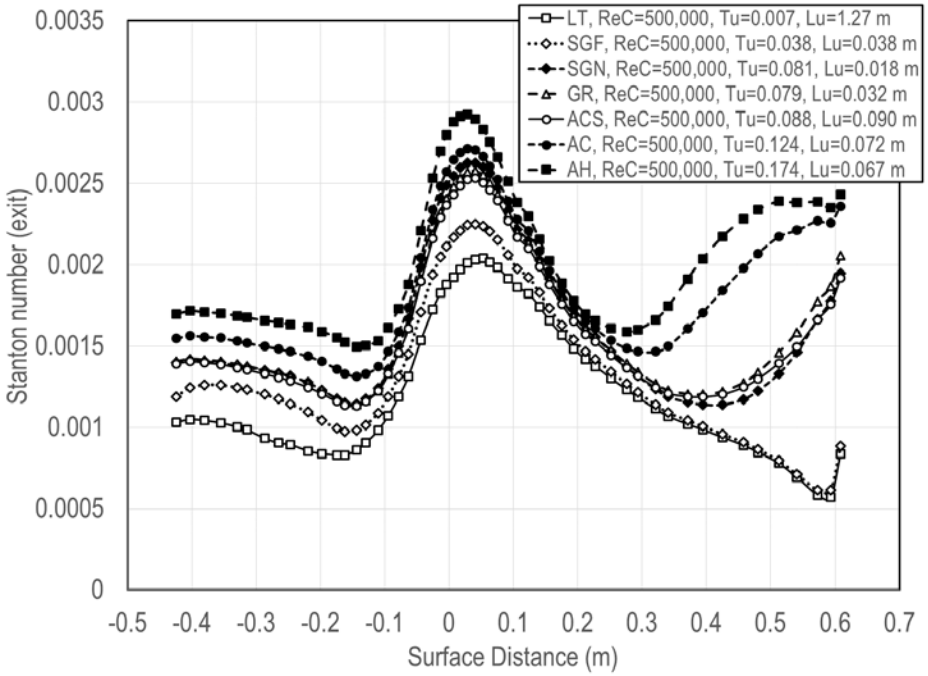

MIDSPAN HEAT TRANSFER DISTRIBUTIONS

- At the 1,000,000 and 2,000,000 Reynolds number we see the transition moving forward on the suction surface with increasing Reynolds number.
- The relative heat load on the leading edge drops well below the turbulent suction surface at Rec = 2,000,000.
- Transition seems to appear on the downstream pressure surface at the higher turbulence levels at 1,000,000 Reynolds No. and it is present at all higher turbulence levels at 2,000,000
- The six elevated turbulence levels show significant augmentation of laminar heat transfer

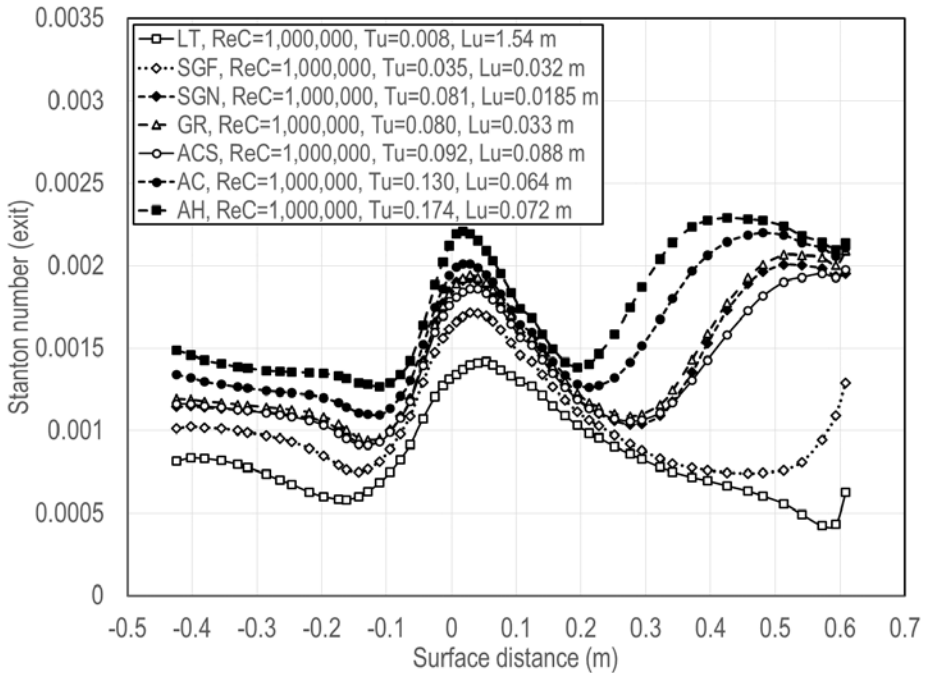

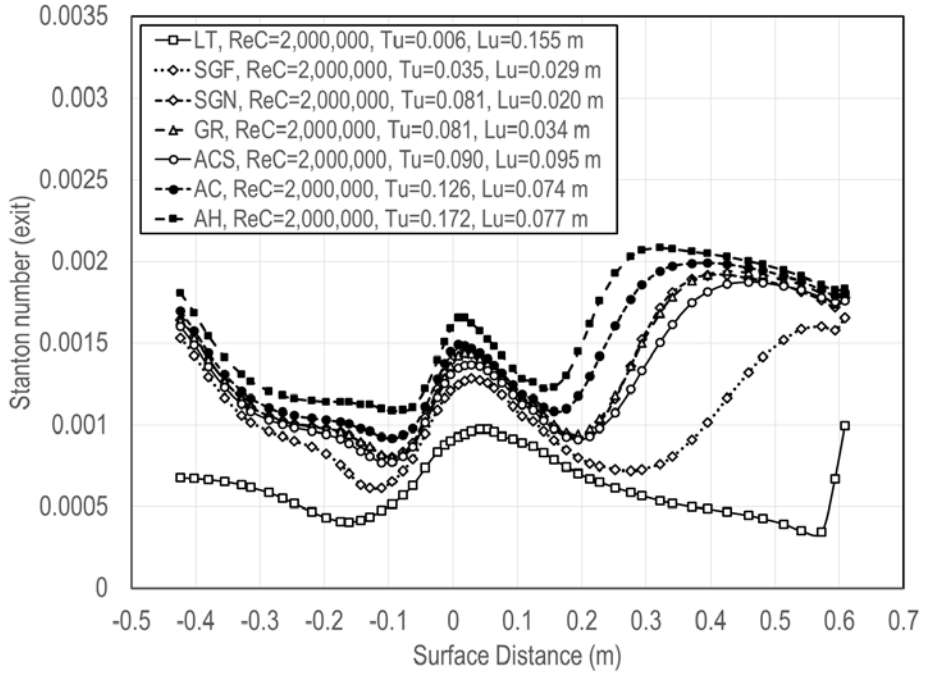

MIDSPAN HEAT TRANSFER DISTRIBUTIONS

- Streamwise acceleration levels are very high in the stagnation region but drop on the suction surface and the near pressure surface.
- After the initial drop on the pressure surface, high acceleration is reestablished downstream.
- Peak augmentation occurs in the leading edge not including transition.
- Augmentation levels continue to fall on the suction surface prior to transition indicating the influence of convex curvature.
- After the initial drop, augmentation levels rise on the pressure surface while transition criteria is initially

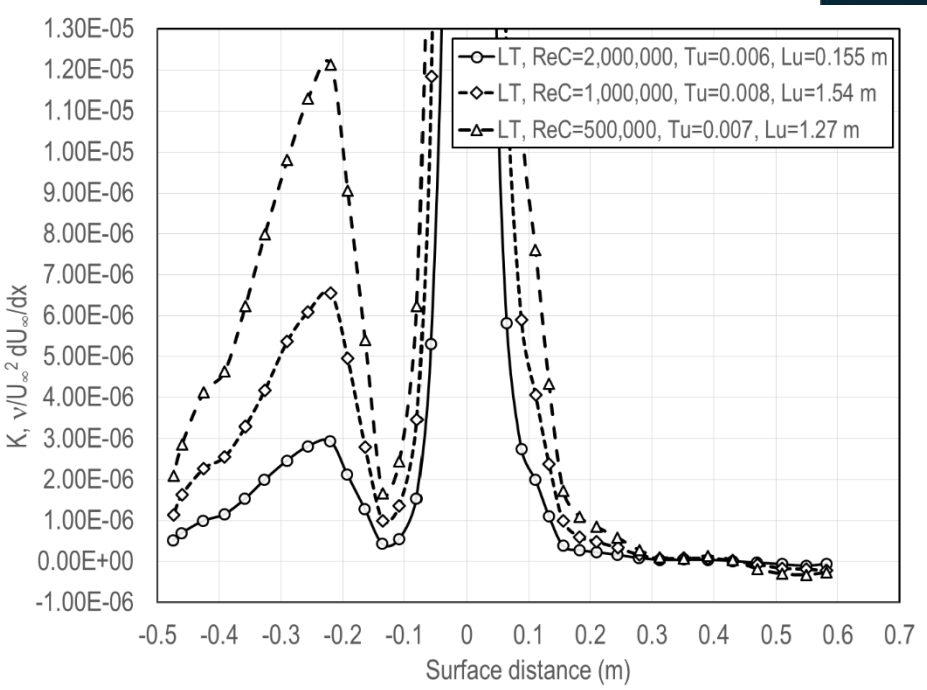

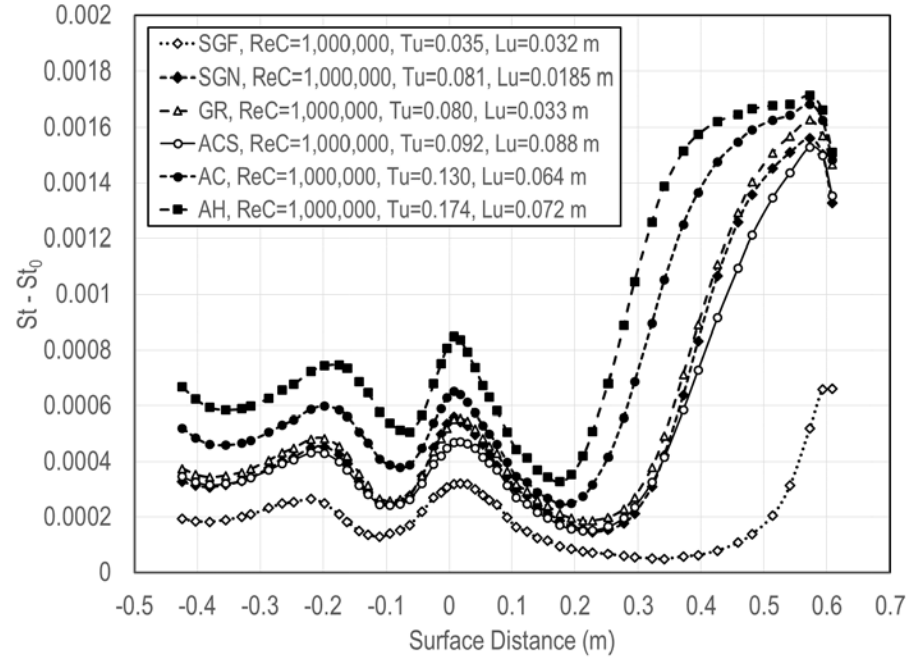

MIDSPAN HEAT TRANSFER DISTRIBUTIONS

- Boundary layer predictions show reasonable agreement with laminar augmentation except in the leading edge where it is significantly low.
- Transition on the suction surface is predicted early probably due to a delay caused by convex curvature.
- Pressure surface predictions show some difficulty with augmentation and transition.
- Stagnation region augmentation levels drop increasingly below the TRL parameter as the pseudo time scale (Lu/Tu) decreases.

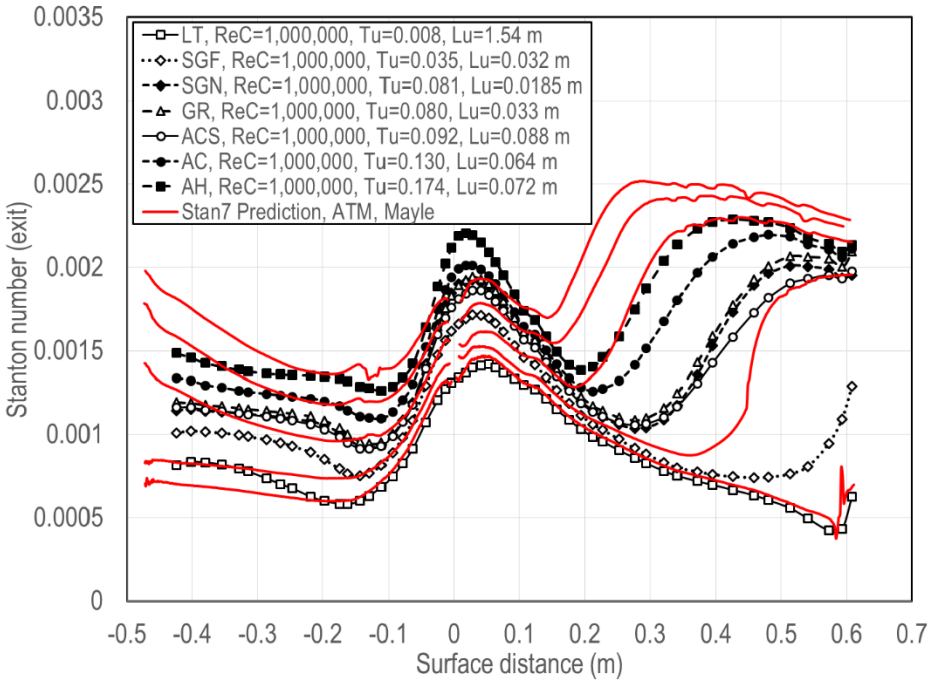

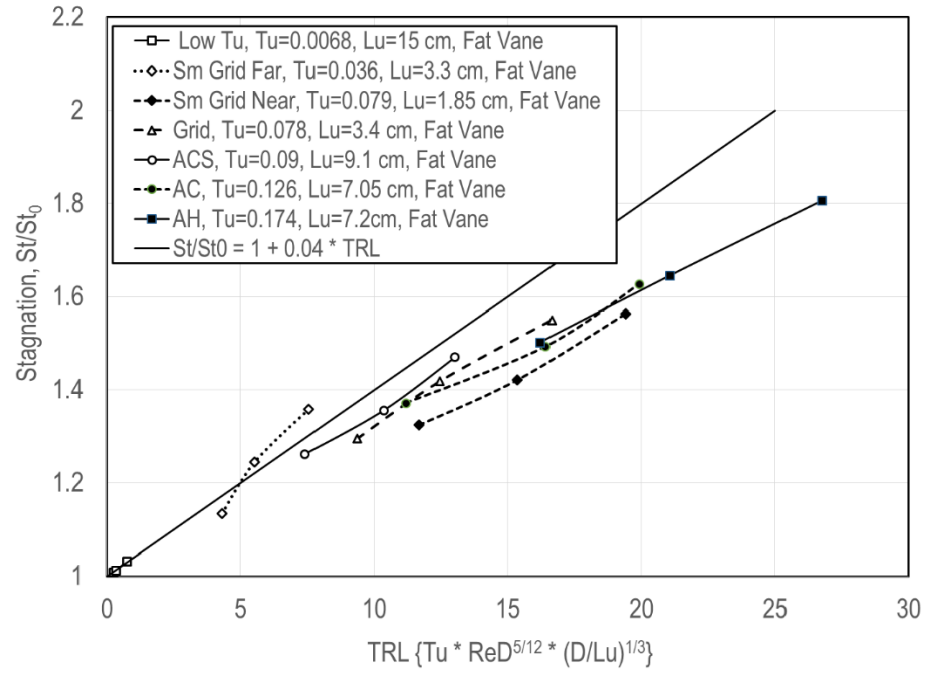

Full surface vane suction surface heat transfer

- UND's large scale cascade provides thermal camera access to the suction surface through a tailboard which integrates zinc selenide windows.
- For full surface heat transfer measurements the vane is painted black and reflective dots are painted on the surface to provide physical reference points.
- Infrared images in the 8 to 13 μm range are acquired for the heated and unheated conditions.
- Midspan temperatures acquired at the same time as IR images are used for in situ calibration.

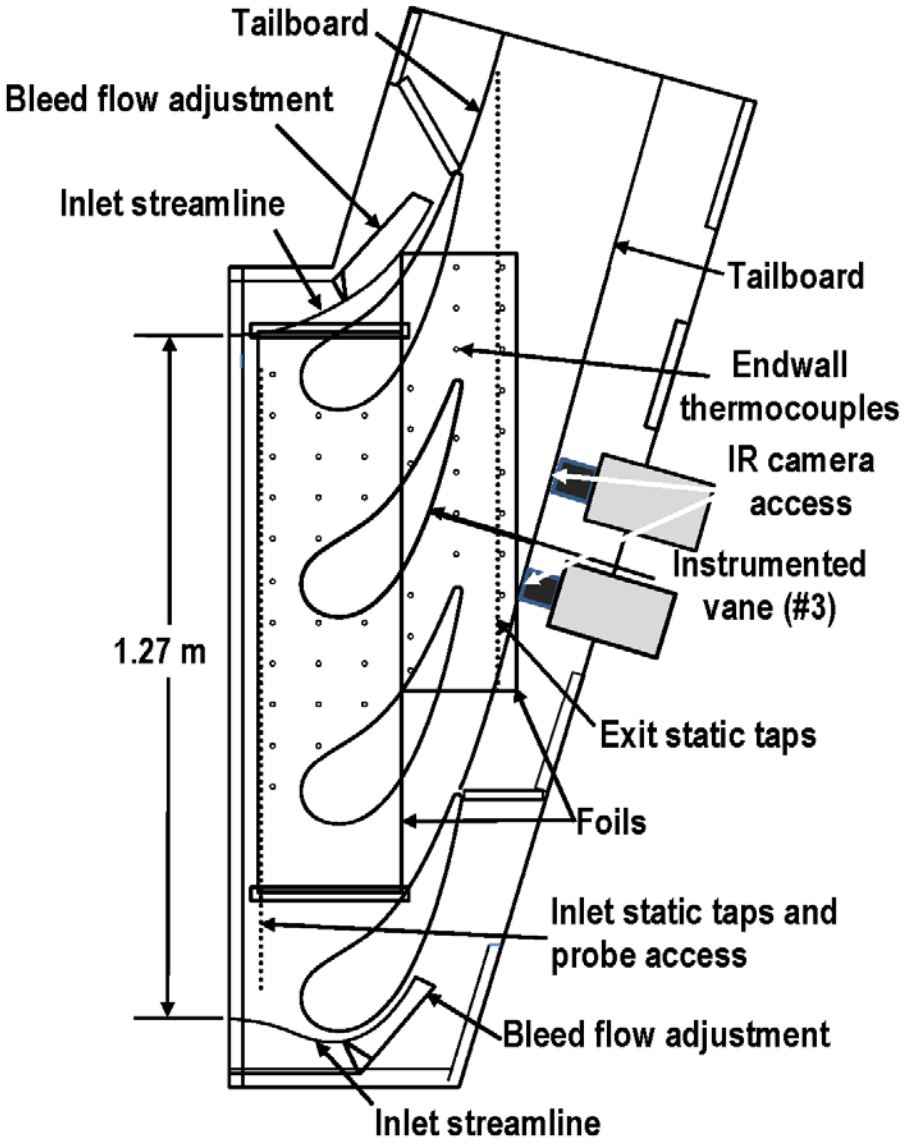

SUCTION SURFACE HEAT TRANSFER DISTRIBUTIONS

- The raw infrared image shows the start of heating on the left as well as the trailing edge of the vane and the vane/endwall interface.
- The reflective spots visually show on the thermal image providing physical mapping information for the heat transfer distribution.
- Both the image in general and the dots show the fisheye effect of the camera which can be adjusted.
- A comparison of the midspan thermo-couples with the IR temperature values at the same span with and without heating allow for an in situ calibration.

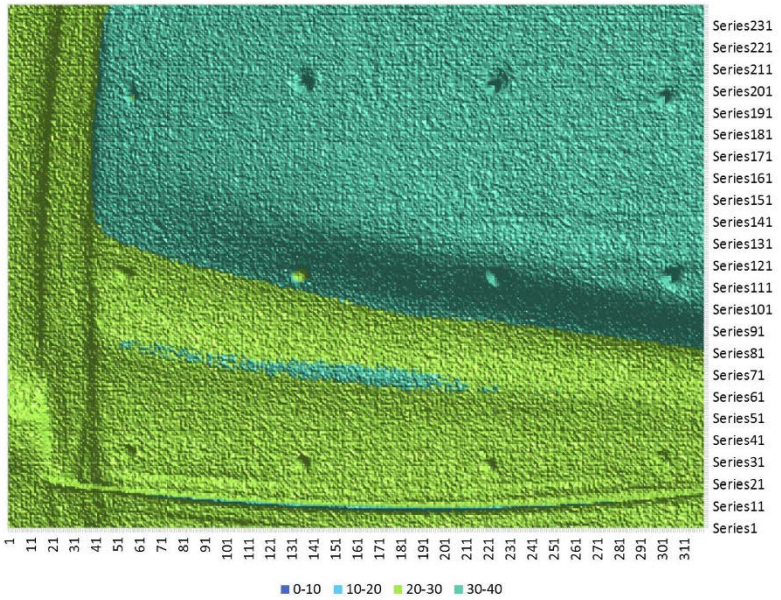

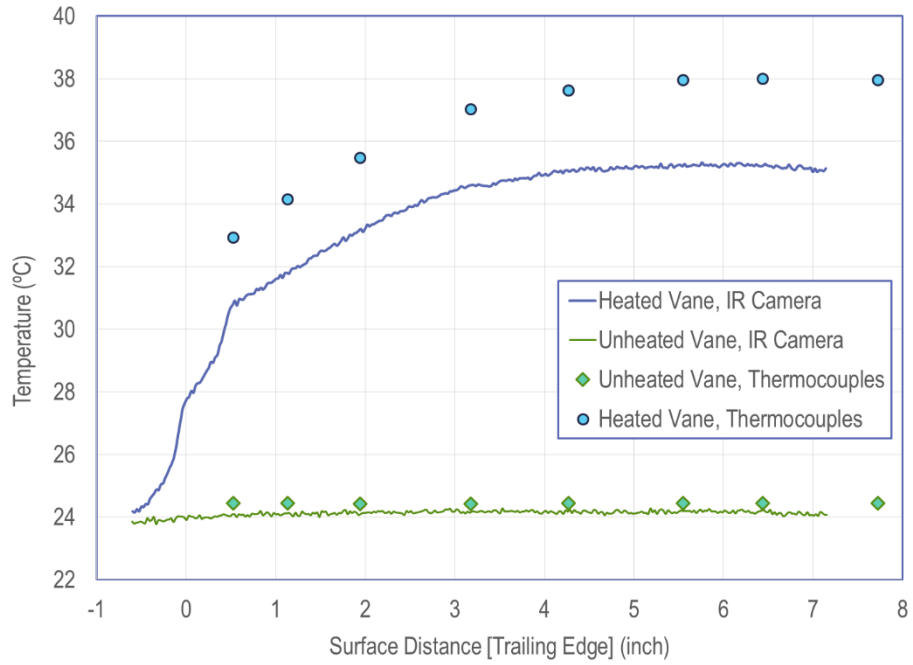

Midline comparison of heated and unheated temperatures, thermocouple vs. IR camera.

SUCTION SURFACE HEAT TRANSFER DISTRIBUTIONS

- The midspan heat transfer distribution for the black painted vane was compared with the distribution acquired using the bare foil heater.
- The agreement between the two heat transfer distributions provides confidence in the radiation losses.
- The initial heat transfer image shows significant graininess in spite of averaging over three pictures.
- The heat transfer distribution also shows the location of the reflective dots as well the extent of the secondary flows as they move off the endwall and up onto the suction

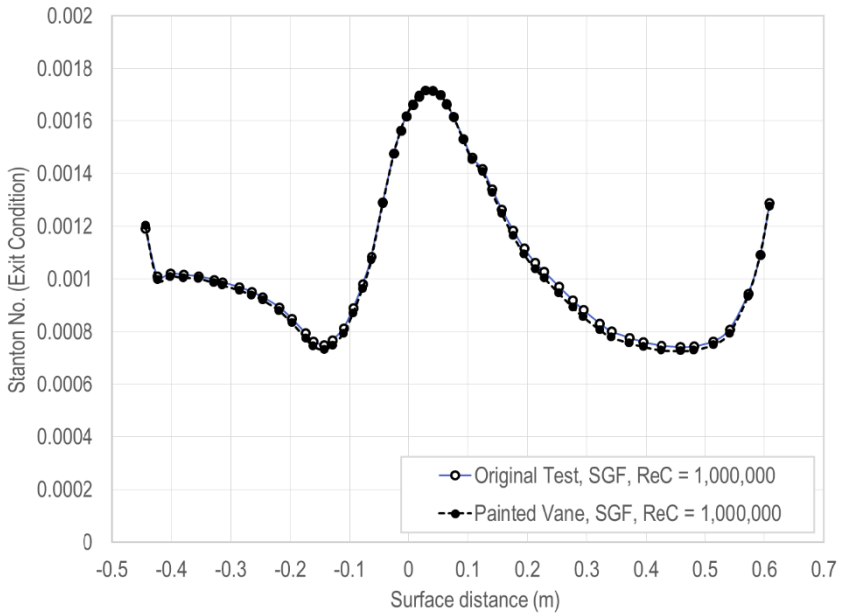

Comparison between metal foil surface and painted surface heat transfer distribution.

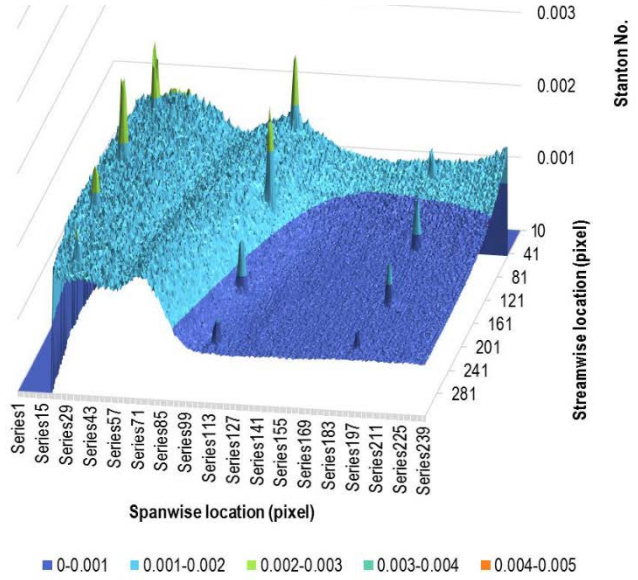

Contour plot of suction surface Stanton No. distribution with heated endwall, no smoothing, Re_C = 1,000,000, SGF.

SUCTION SURFACE HEAT TRANSFER DISTRIBUTIONS

- The array of Stanton numbers was smoothed in both the streamwise and spanwise directions to eliminate much of the graininess of the image.
- The asymmetry of the heat transfer can be seen in the image due to the stronger secondary flows on the unheated endwall due to the window.
- The fisheye effect of the acquired IR image can be adjusted with a simple geometric transformation.
- The resulting image displays a straight edge along the endwall and will allow the top image and bottom image of a heat transfer run to be merged together as one image.

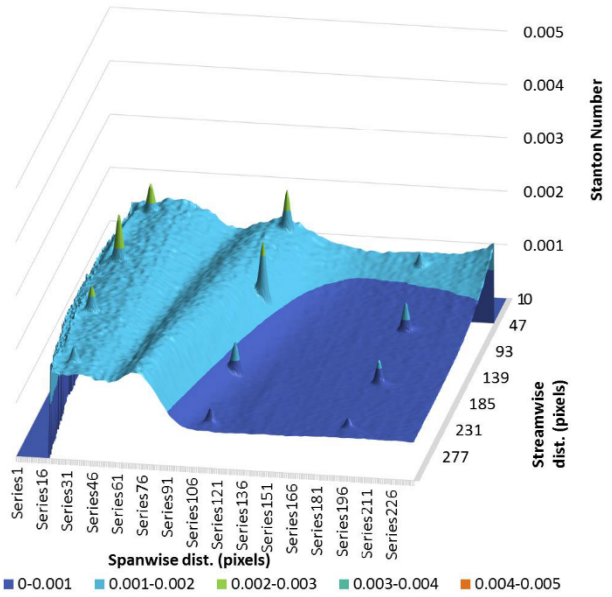

Contour plot of suction surface Stanton No. distribution with heated endwall, with smoothing, Re_C = 1,000,000, SGF

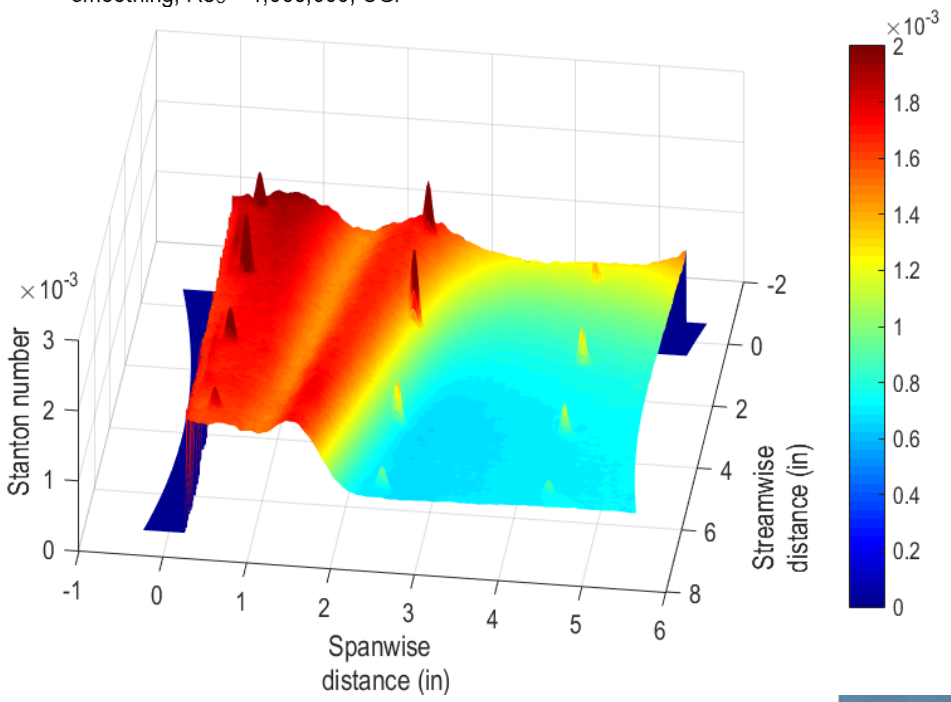

SUCTION SURFACE HEAT TRANSFER DISTRIBUTIONS

- When air moves off the unheated endwall onto the heated suction surface it produces a significant unheated starting length effect.
- In spite of smoothing, the Stanton No. values at the edge of the suction surface are ragged due to the low surface to air temperature difference.
- The data acquired from the lower camera position catches the beginning of the secondary effects.
- The relatively high heat transfer in the region influenced by the secondary flows is highly visible due to the relatively low local heat transfer .

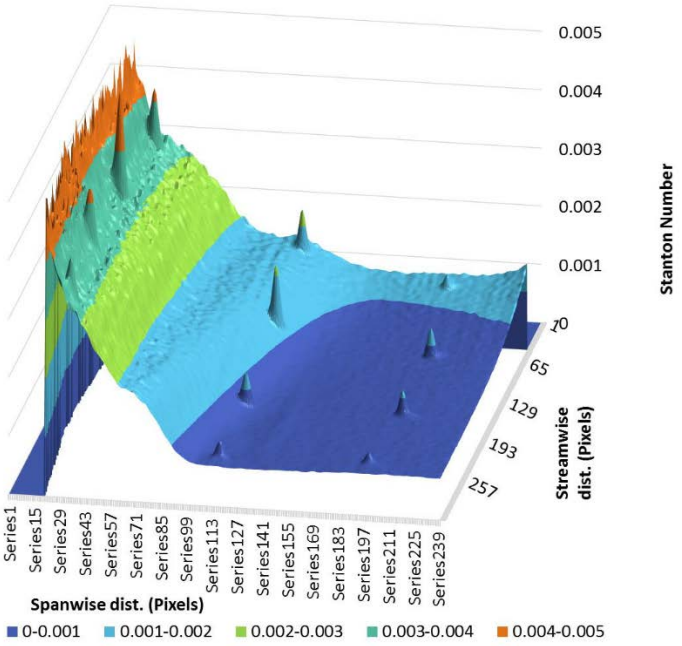

Suction surface heat transfer distribution with no endwall heating, SGF, Re_C = 1,000,000, top position.

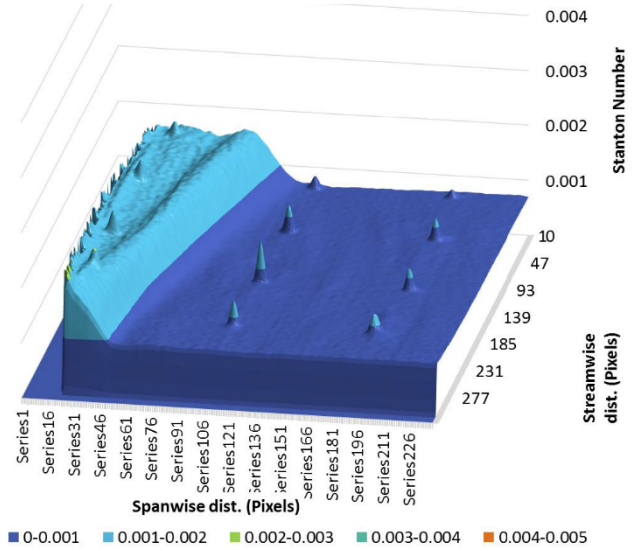

Suction surface heat transfer distribution with endwall heating, SGF, Re_C = 1,000,000, bottom position.

SUCTION SURFACE HEAT TRANSFER DISTRIBUTIONS

- Spanwise distributions of Stanton No. show a large variation in the midspan area with turbulence but a much smaller difference in the region affected by secondary flows.
- The dip in Stanton number at a span of around 1.6 inches for the LT and SGF cases may indicate the separation line of the passage vortex.
- The data acquired at the higher turbulence levels show higher heat transfer in the midspan area.
- The evidence of discrete vorticity is much less dominate at the higher turbulence levels due to aggressive mixing and unsteadiness.

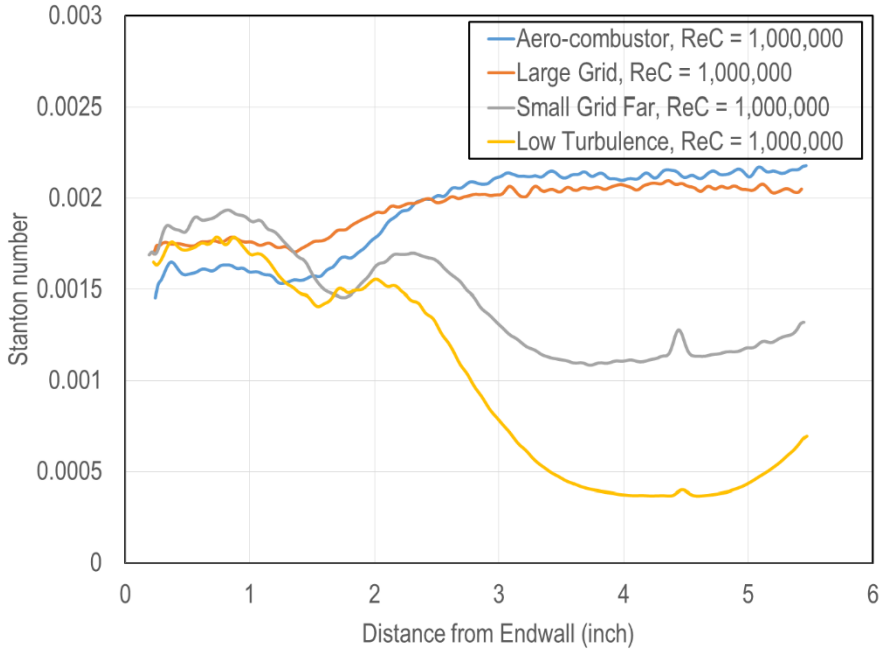

Comparison of spanwise surface heat transfer distribution as a function of turbulence level.

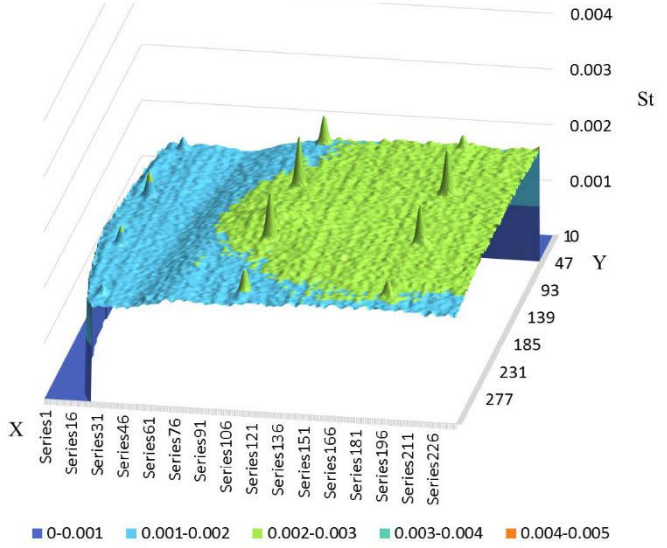

Stanton number distribution downstream suction surface with endwall heating, large grid, Re_C = 1,000,000.

VANE FILM COOLING AND HEAT TRANSFER DISTRIBUTIONS

- Suction surface heat transfer distributions are complete.
- Preparations are being made to fabricate a heat transfer vane which integrates film cooling plenums.
- A solid model of the suction surface film cooling plenum integrated into the profile of the vane shows the flow geometry as well as the plenum pin arrays.
- Pressure surface film cooling and heat transfer will be acquired using surface thermocouples while suction surface distributions will be acquired with both surface thermocouples and IR camera measurements.

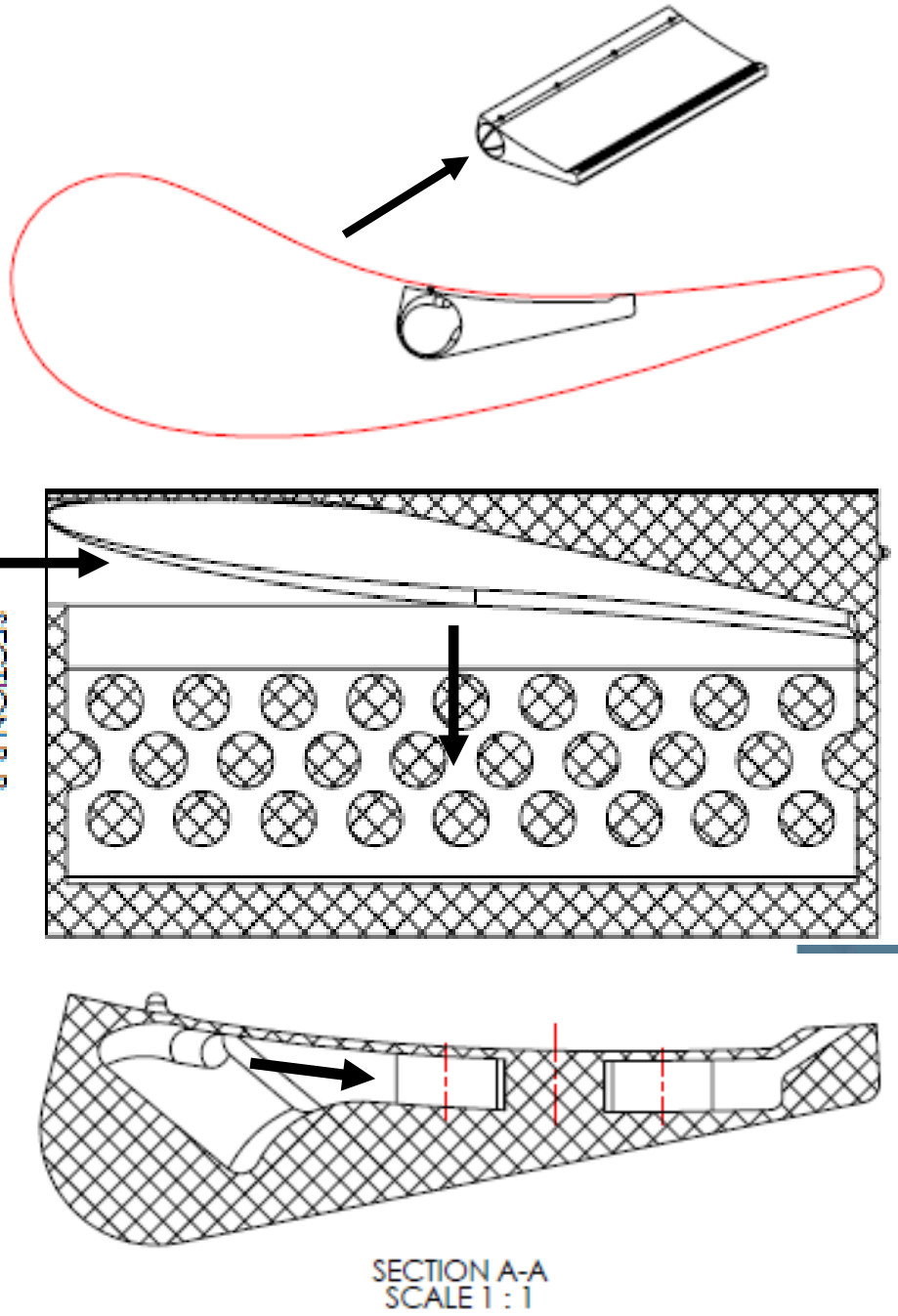

INTERNAL COOLING INVESTIGATION

This bench scale internal cooling, flow and heat transfer rig, has been used for investigating configurations of incremental impingement and will be used for converging high solidity arrays and counter cooling,. The internal cooling rig includes a high pressure blower driven with a variable frequency drive, a plenum with heat exchanger, an orifice tube, a downstream diffuser section and a flow conditioning section flow or screen box.

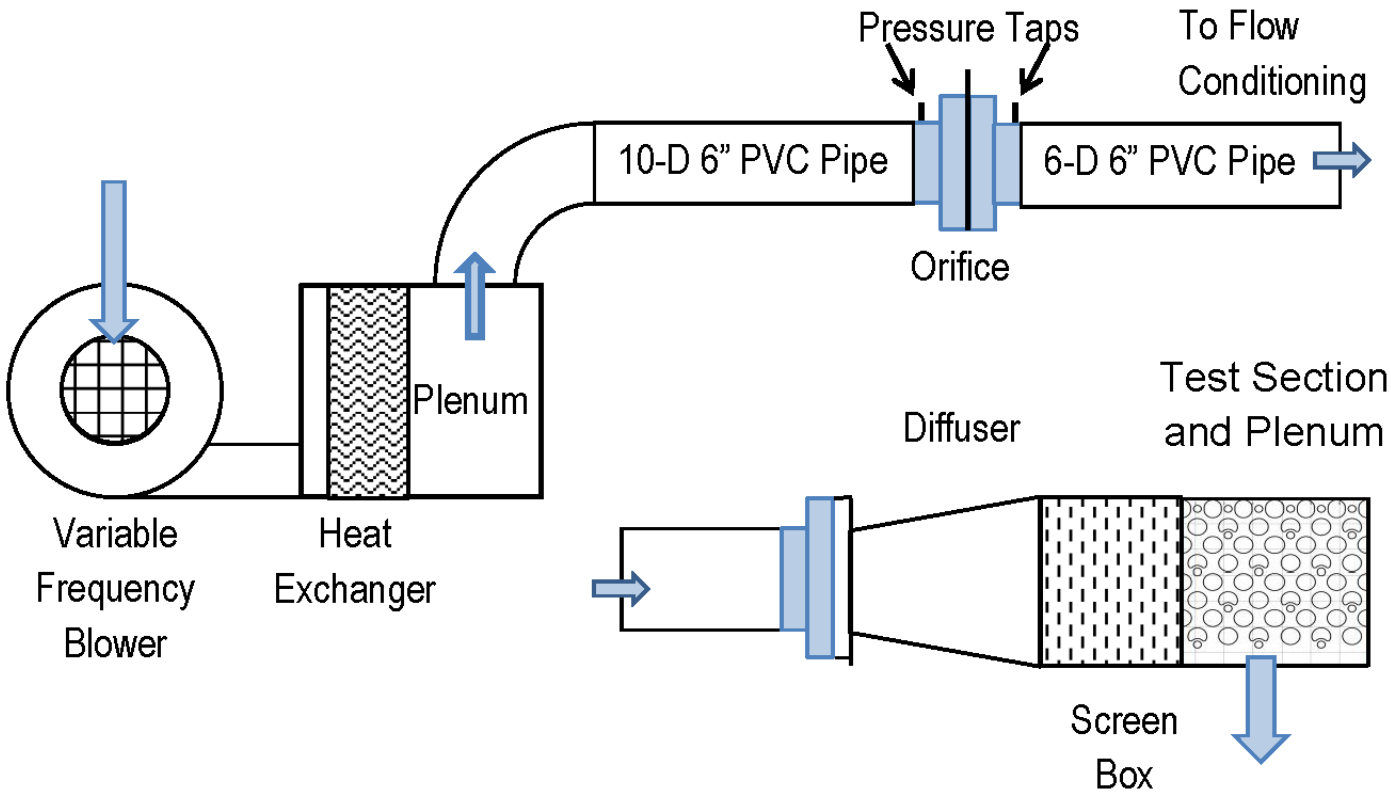

INCREMENTAL IMPINGEMENT GEOMETRY

Testing has included relevant inlet and exit geometries along with variable hole size to allow a significant variation of the cooling hole distribution for a given application. Testing has included 26 different hole configurations out of 29 planned.

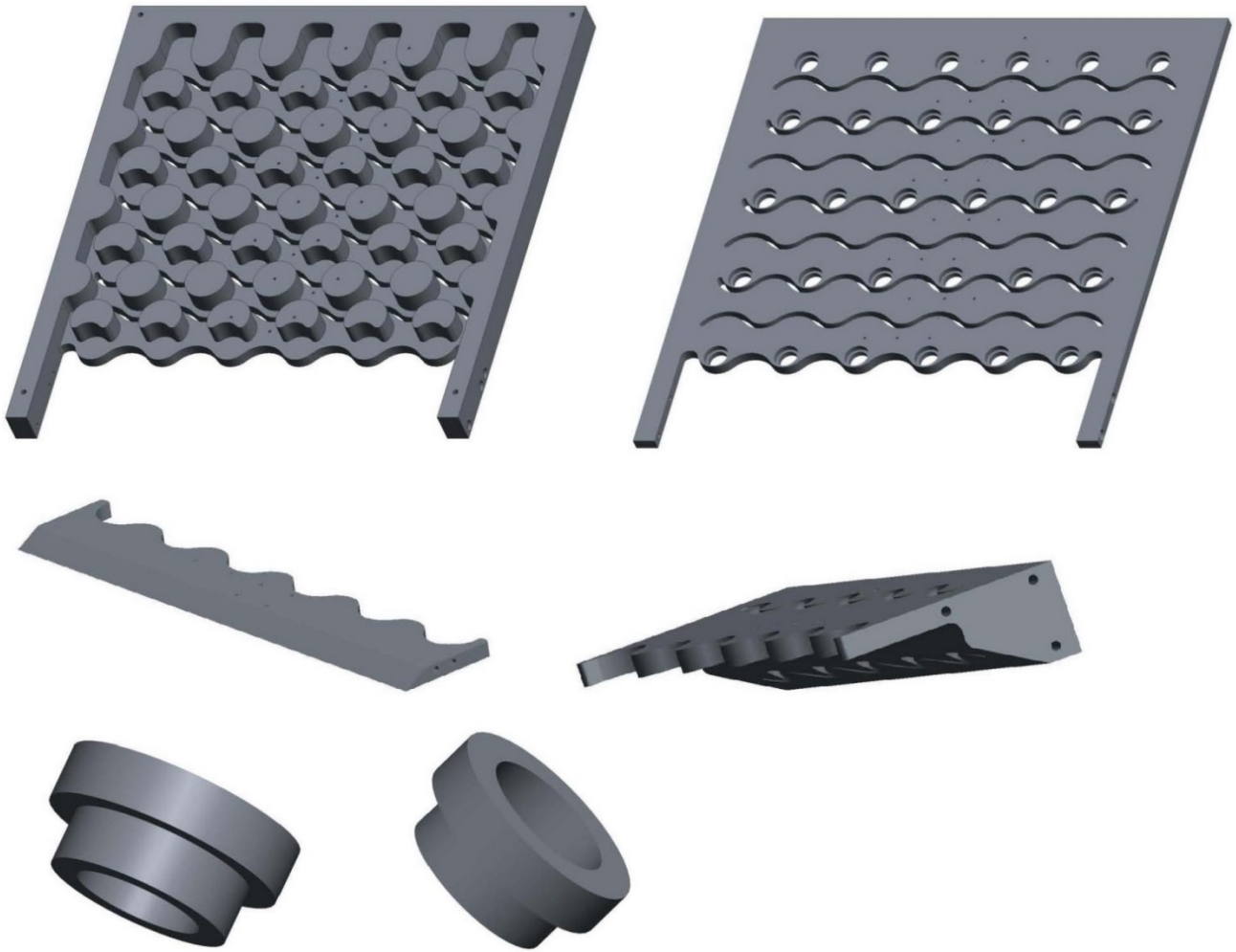

INCREMENTAL IMPINGEMENT WITH VARIABLE HOLE SIZES

- Heat load can vary over the surface of a component, while conventional cooling methods have limited ability to vary locally.
- The heat transfer distribution around the stagnation region for the current vane design is presented in the top figure.
- The cooling parameter data shown below is for the earliest configuration for incremental impingement, LSSSS.
- While this cooling method keeps a high level of cooling across the array it does not match the needed heat load very well.
- Variable hole size incremental impingement is clearly needed.

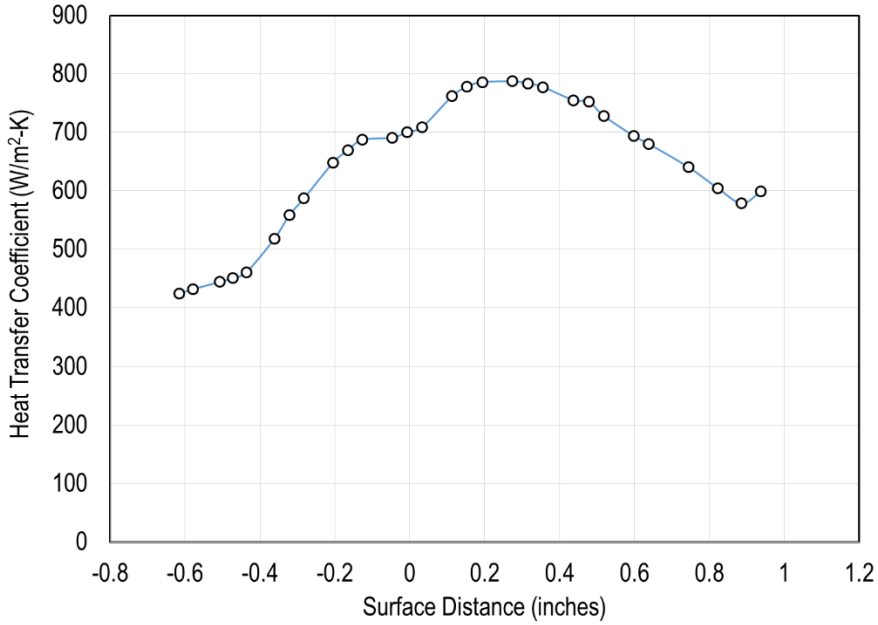

The predicted heat transfer loading distribution for warm cascade vane in the stagnation region and near suction surface.

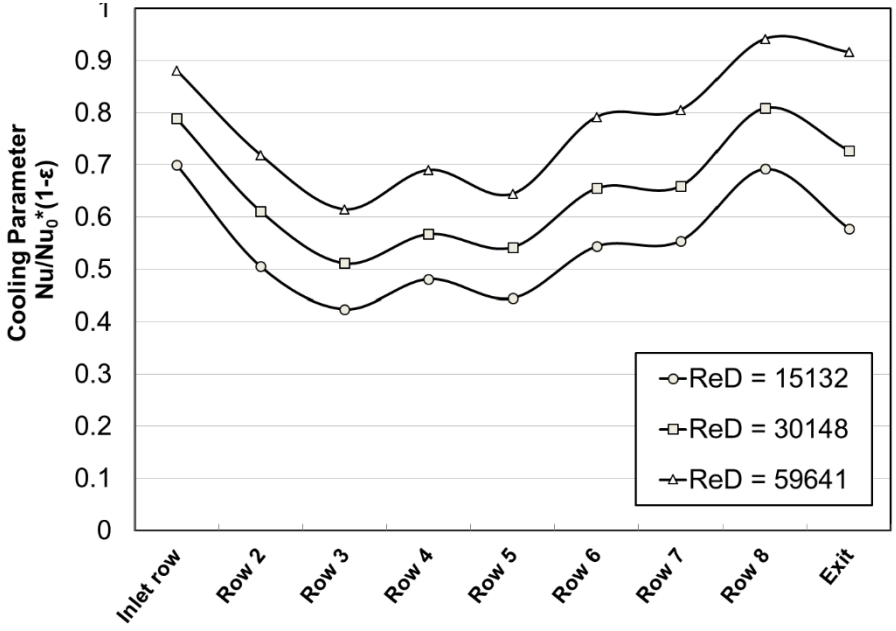

The influence of Reynolds number on cooling parameter, $(1-\varepsilon)^* Nu/Nu_0$, LSSSS.

INCREMENTAL IMPINGEMENT WITH VARIABLE HOLE SIZES

- The first approach for variable hole size incremental impingement used small medium and large hole sizes.
- The array had only a minimal ability to vary cooling level due to a significant amount of blockage in the downstream region as more flow entered the array.
- The dimensionless pressure drop distribution shows that much of the pressure loss occurs downstream due to the flow around the high solidity pedestals.
- The overall array pressure drop is very much dependent on the total impingement hole area.
- It was obvious that we needed to add smaller hole sizes for more flexibility.

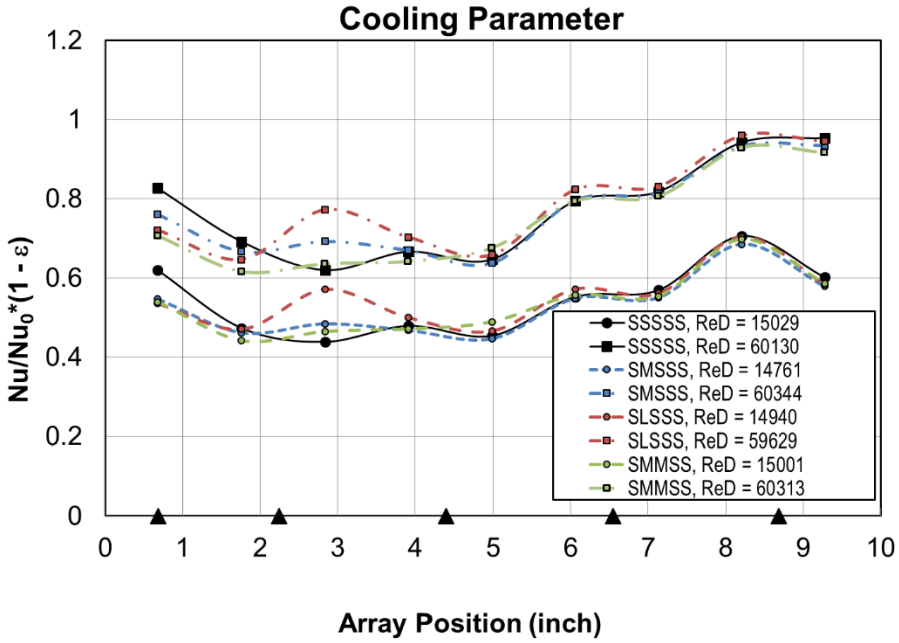

The influence of second hole size on cooling parameter, $(1 - \varepsilon)^* Nu/Nu_0$ for S, M & L

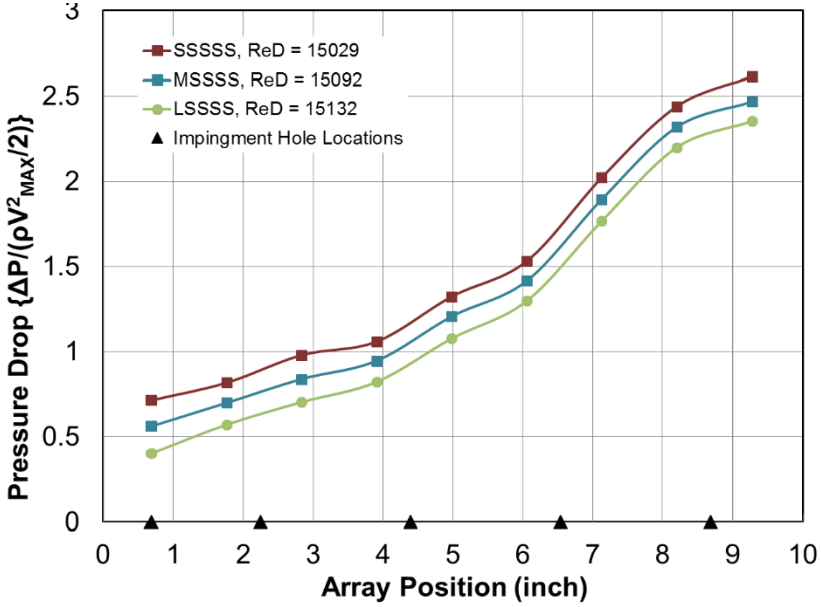

Dimensionless pressure distributions versus array location showing influence of inlet hole area and the significant crossflow pressure drop.

INCREMENTAL IMPINGEMENT WITH VARIABLE HOLE SIZES

- Adding a petite hole size provided significantly more flexibility in addressing variable heat load.
- The current array is designed to put impingement holes behind pedestals in rows 2, 4, 6, and 8 in addition to the first row of pedestals.
- However, in principle a hole can be placed behind any pin in the array .
- Although our current configuration is not ideal to match our current heat load in the leading edge, it is improved.
- The current database should be sufficient to ground the developing analytical tool giving more flexibility.
- Petite holes give a high pressure drop but total hole area can be managed.

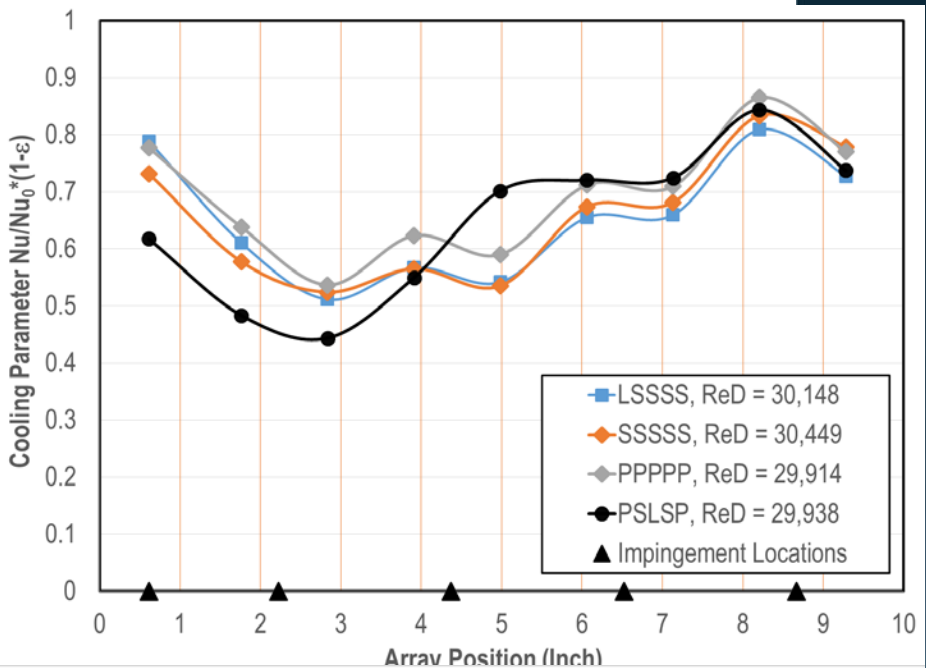

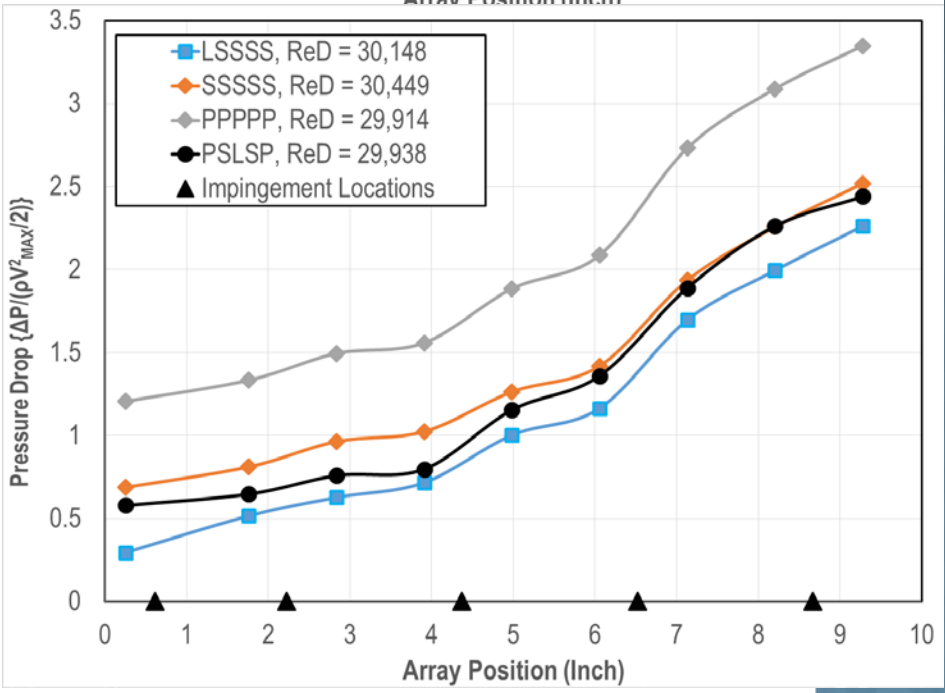

CONVERGING DIAMOND PEDESTAL TRAILING EDGES

- A converging diamond pedestal array was initially proposed to cool the trailing edge.
- The finite difference and FEA analyses indicated a trailing edge effectiveness which was lower than the initial goal.
- A second array was designed with one fewer rows of pedestals and a trailing edge region opened to allow more flow.
- We plan to test both arrays to confirm our correlation with an abrupt expansion and document any differences.
- The 8 row diamond pedestal array is instrumented and ready for testing.
- The tests are planned to begin shortly after completing the current IP tests.
- There are 2 current configurations.

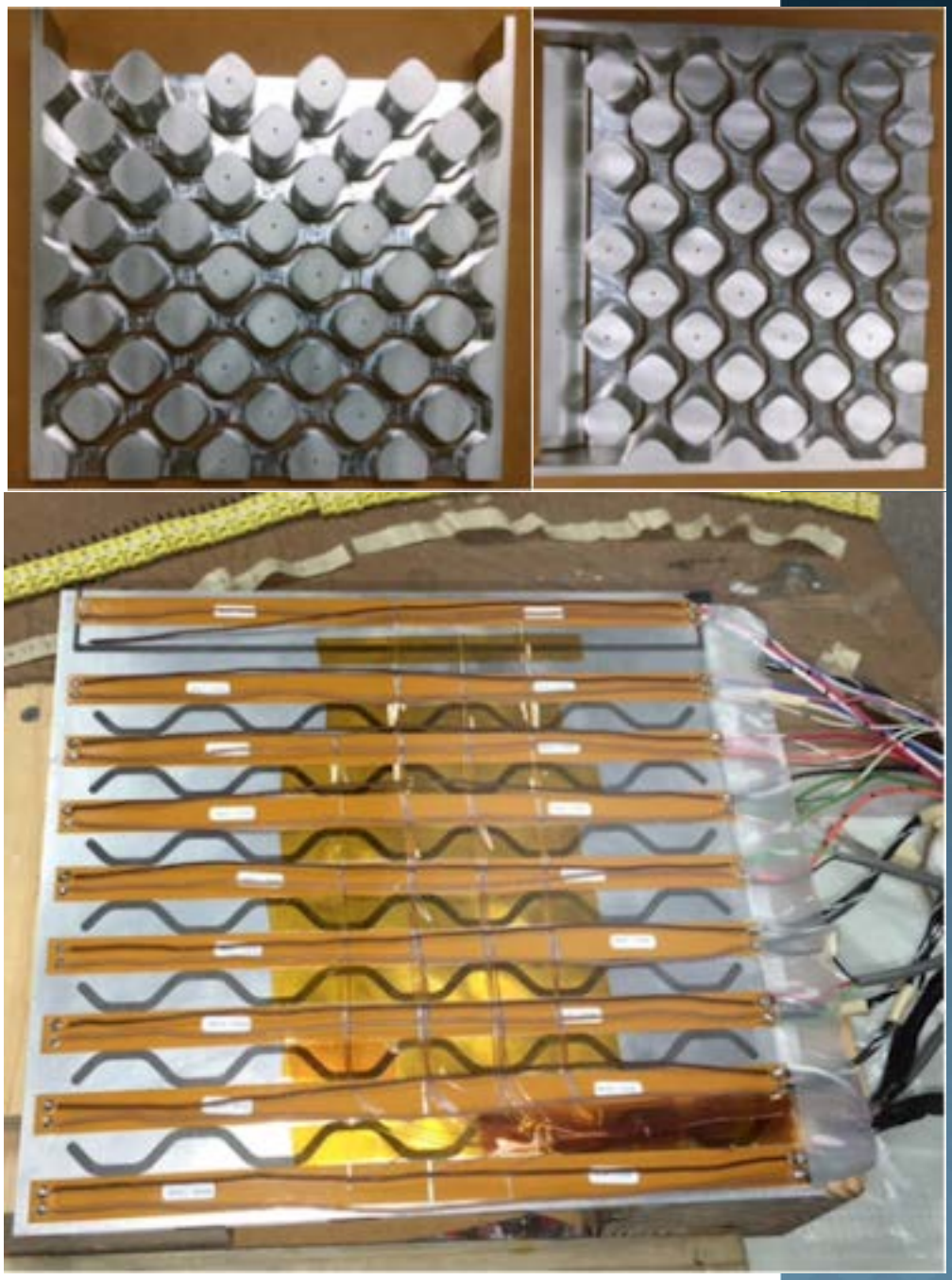

Computational Research Plan

- Goals:
  - Develop a suite of HTC correlations that serve as input for a predictive design tool
  - Numerical optimization of geometric parameters and cooling design
  - Complement measurements with supporting computations that describe the flow physics
- Tasks:
  - Slot film cooling over a Vane fed by a turbulated plenum-UND data (I-LES)
  - Internal cooling with pedestals and incremental coolant impingement-UND data (II-LES)
  - Low speed cascade flow simulations (III)
    - RANS/LES/DES with isoflux uncooled walls-UND data (IIIa)
    - LES/DES with slot cooling
  - High speed hot cascade flow simulations (IV)
    - RANS validation with existing vane data
    - RANS w/ new vane- aero and HT with internal HTC correlations
    - Predictive design tool with internal and external correlations

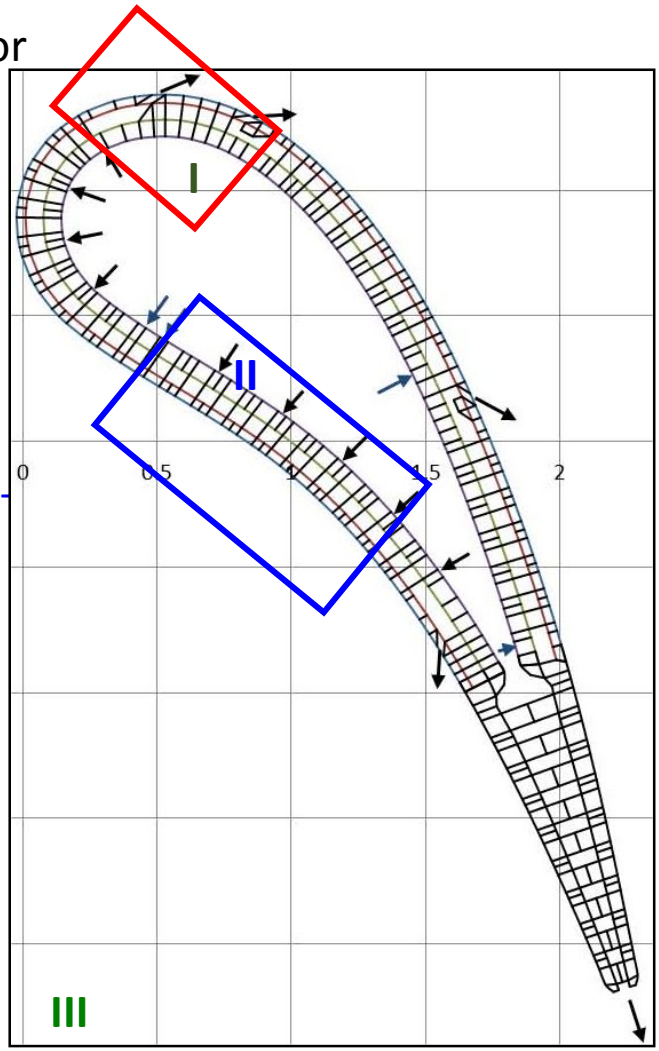

I-Slot film cooling over a Vane fed by a Turbulated Plenum-Strategy

- Goals:
  - Cooling effectiveness (η) and HTC correlations that serve as input for a predictive design tool
  - Complement measurements with supporting computations that describe the flow physics

I-A-Slot cooling on Flat Plate*

✓ **Freestream turbulence effects**
- No Acceleration
- No Leading edge effect
- No slot turbulence (i.e. no pin fins)

I-B-Slot cooling on Flat Plate with slot Turbulence**

- **Freestream turbulence**
- No Acceleration

✓ **Effect of slot turbulence**

I-C Slot cooling with acceleration-UND data***

- **Mainstream turbulence**

✓ **Acceleration**

✓ **Leading edge effect**
- **Slot turbulence (i.e. Pin fins upstream of slot)**

*J.P. Hartnett, R.C. Birkebak, E.R.G. Eckert, J. Heat Transfer. 83 (1961) 293–305.

I- Slot cooling over full cascade
- Mainstream turbulence
- Acceleration
- Leading edge effect
- Pin fins upstream of slot

**R.S. Bunker, A Study of Mesh-Fed Slot Film, J. Turbomach. 133 (2011) 011022,1-8.

***Busche, M L, and F E Ames. 2014. "Slot Film Cooling Measurements on an Accelerating Test Surface Subjected a Range of Turbulence Conditions." In *Proceedings of ASME Turbo Expo 2014*,

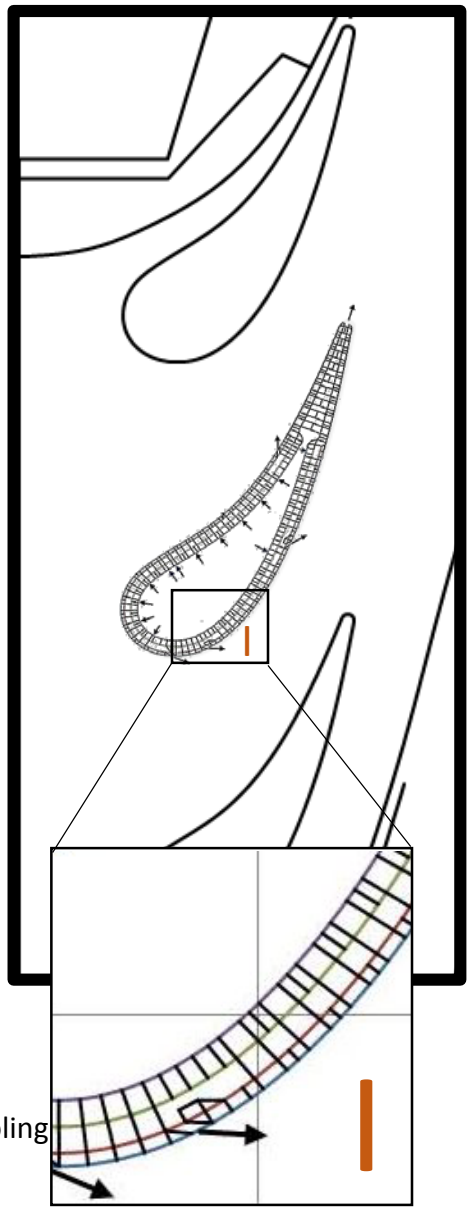

I-A-Slot Cooling over Flat Plate

- Case setup identical to Hartnett et al*

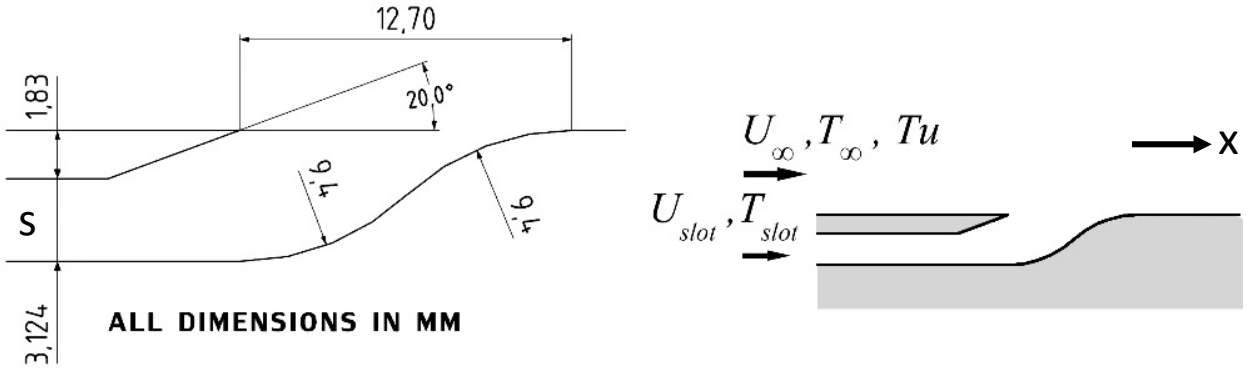

- Turbulent boundary layer upstream
  - Synthetic eddy method (SEM) for inflow generation**
  - Range of upstream turbulence
- Large Eddy Simulation
  - dynamic Smagorinsky SGS model
- Incompressible Navier-Stokes
  - 2nd order scheme
- Grid independence achieved (grid size 6.4 million)

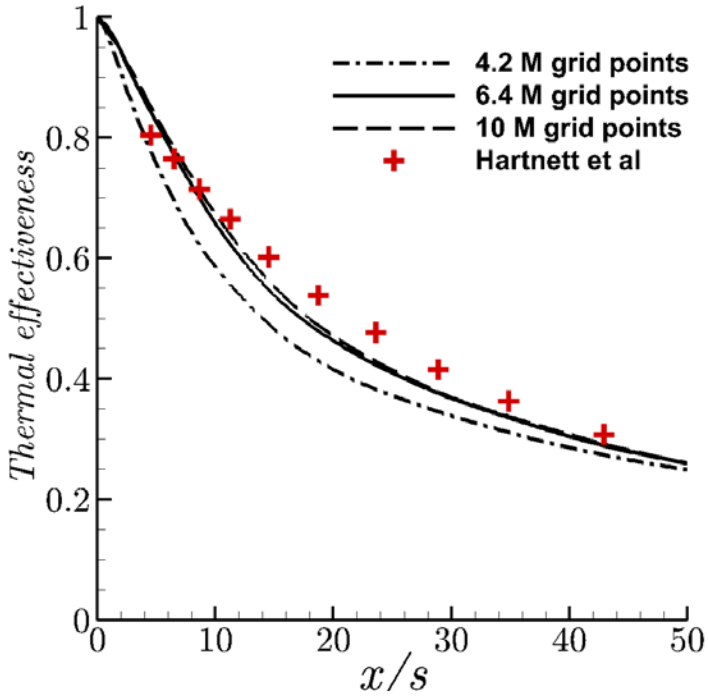

*Hartnett, J. P., Birkebak, R. C., and Eckert, E. R. G., 1961, J. Heat Transfer, **83**(3), pp. 293–305.

Jarrin, N., Benhamadouche, S., Laurence, D., and Prosser, R., 2006, Int. J. Heat Fluid Flow, **27(4), pp. 585–593.

I-A-Slot Cooling over Flat Plate

- Goals:
  - Study the effect of upstream turbulence

Flow Characteristics
Turbulent boundary layer upstream
Various freestream turbulence

Heat Transfer
Adiabatic film cooling eff.
Anamolous behavior at low freestream turbulence

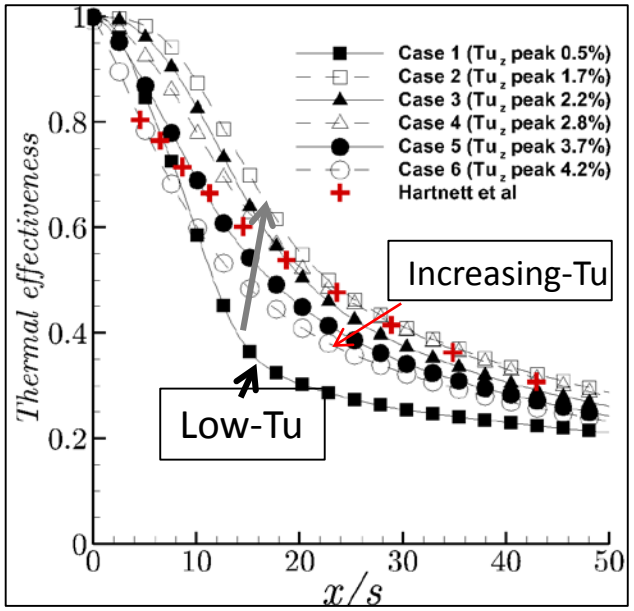

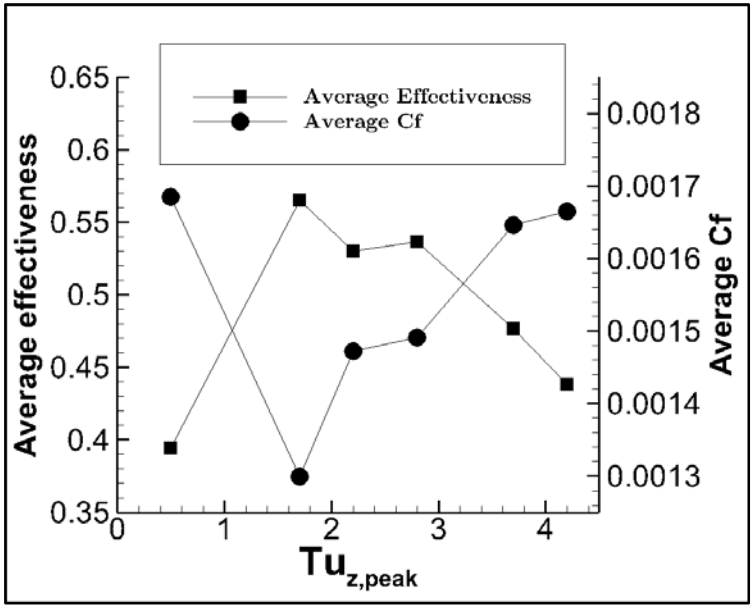

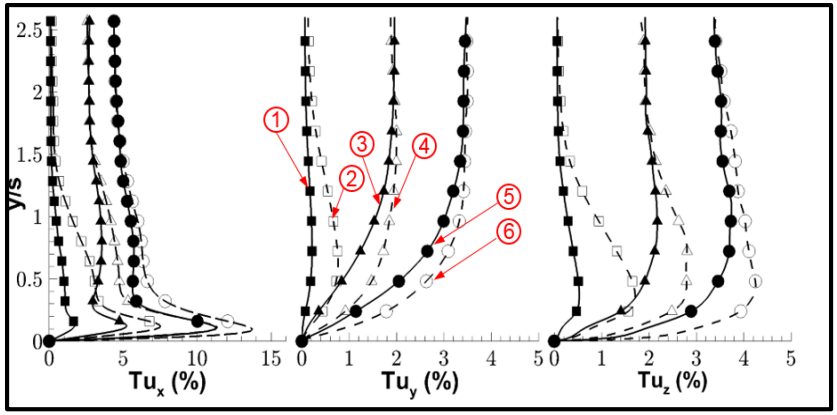

Case	Legend	Tu_{FS}	$K_{peak}/U^2\times10^2$	$Tu_{z,peak}$	$Tu_{x,peak}$	$Tu_{x,fs}$
1	■	0.1%	0.015	0.5%	1.7%	0.1%
2	□	0.1%	0.28	1.7%	7.5%	0.1%
3	▲	3.5%	0.14	2.2%	5.1%	2.6%
4	Δ	3.5%	0.65	2.8%	11.3%	2.6%
5	●	7%	0.65	3.7%	11.2%	4.4%
6	○	7%	1	4.2%	13.6%	4.4%
Hartnett et al	+	N/A	N/A	N/A	N/A	N/A

I-A-Slot Cooling on Flat Plate-Flow Physics

- Observations (low turbulence condition)
  - Formation of Kelvin-Helmholtz vortices (A,B, C etc.) due to the presence of the shear layer
  - Formation of statistically stationary secondary streamwise vortices on braid of K-H (α and β)
  - Very high mixing and fast decay rate of thermal effectiveness due to presence of the K-H and streamwise vortices
  - Distortion of K-H rollers by trapped 3D streamwise vortices
  - Break up to 3D structures downstream

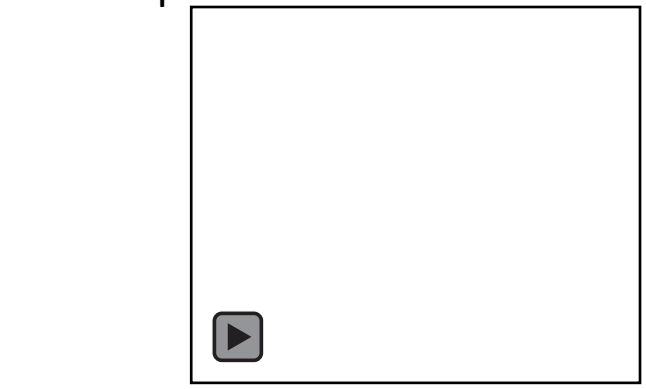

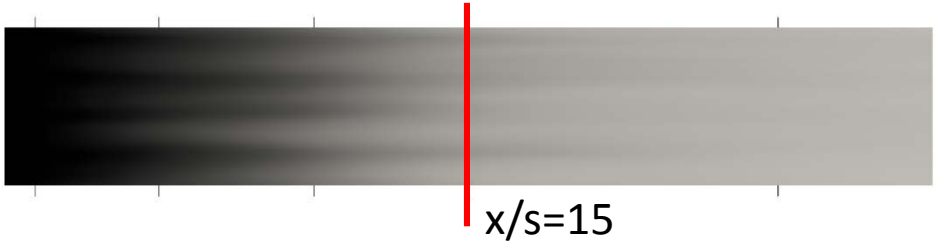

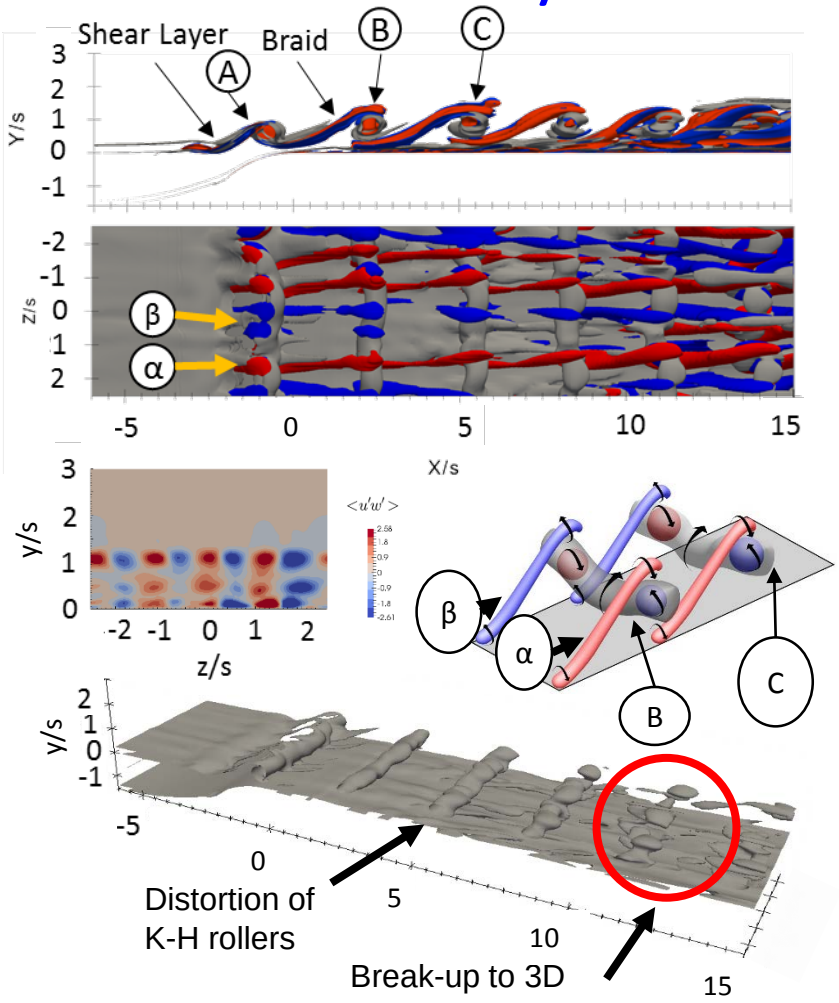

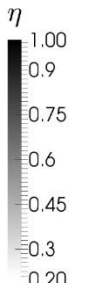

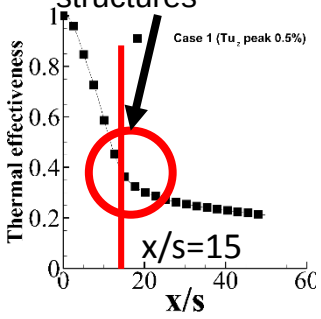

I-A-Turbulence Effect on Film Cooling

- Typically, Thermal effectiveness decreases with turbulence
- Higher turbulence at mainstream alter the K-H and secondary vortices

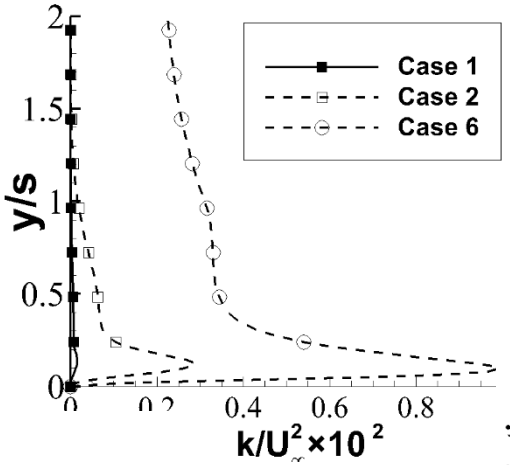

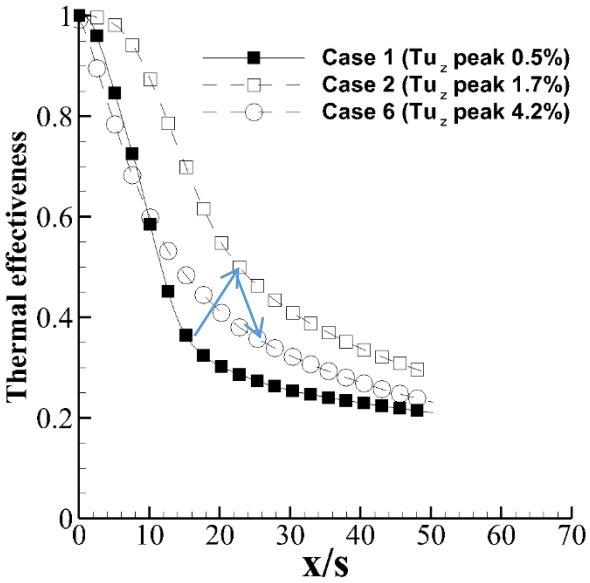

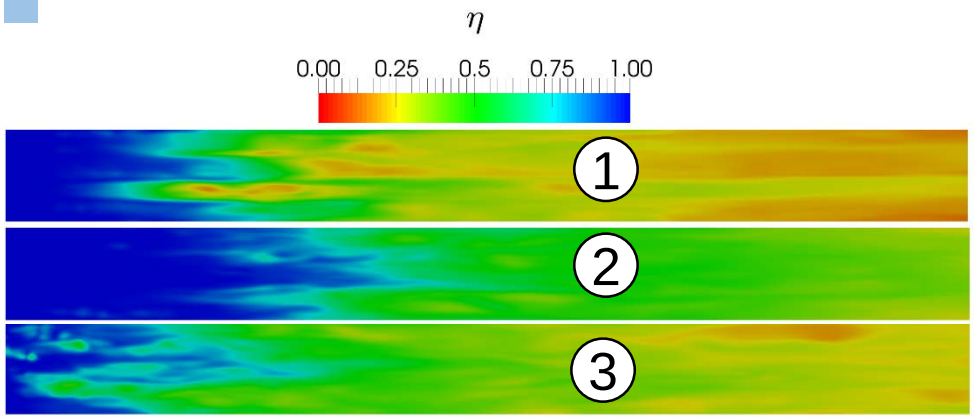

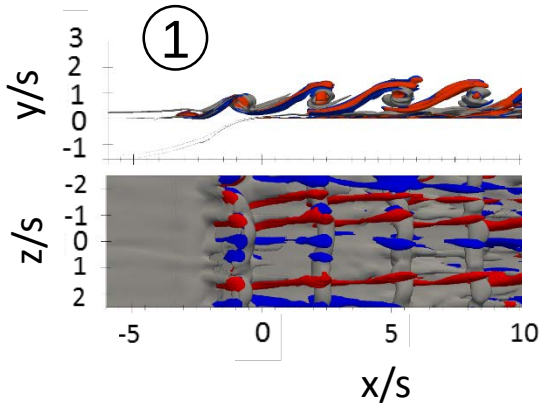

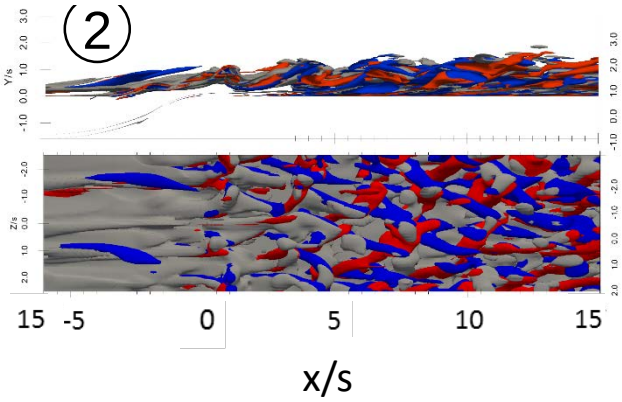

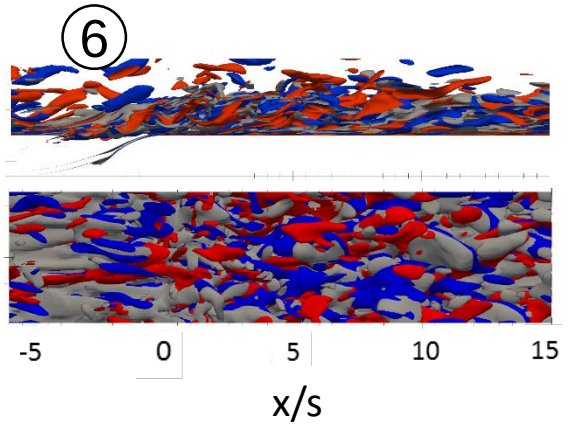

I-B-Effect of Slot Turbulence

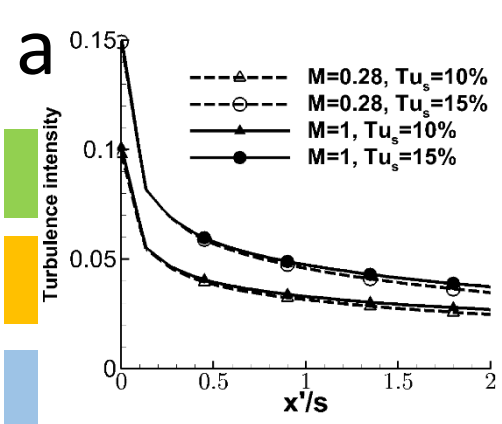

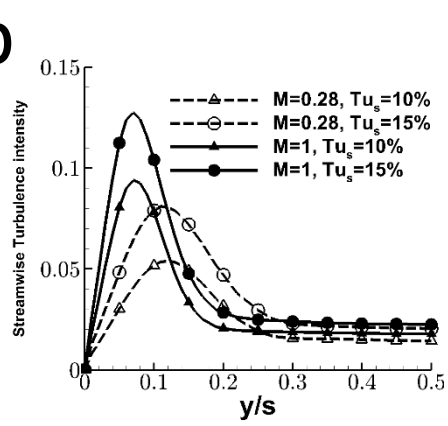

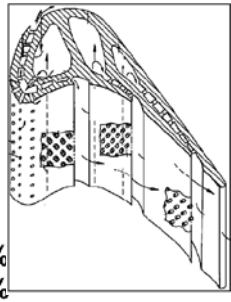

Bunker, 2008

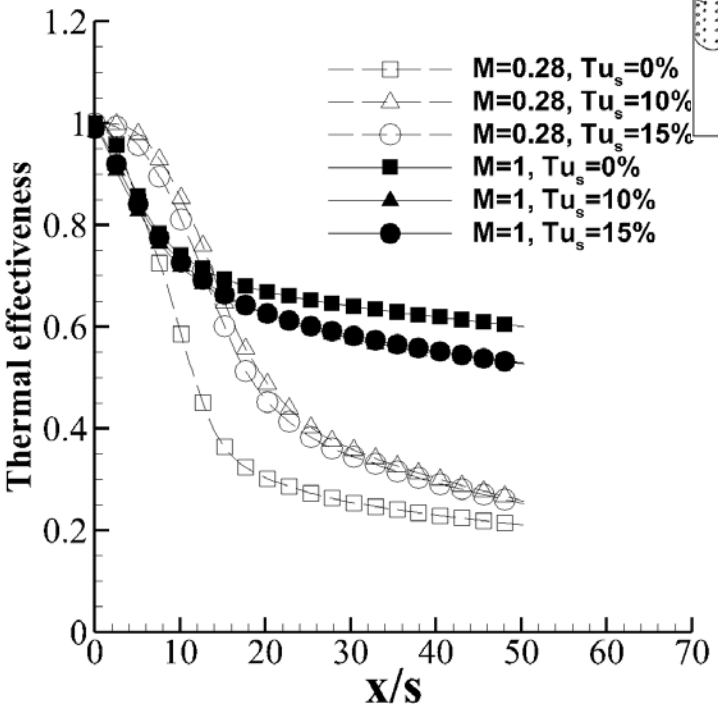

- Various slot turbulence with two different blo ratio (M)
- Low turbulence at mainstream
- Turbulence decay at slot mid-plane (a)
- Turbulence generation near wall (b)

- η initially Increases by adding Tu_s but decreases slightly for higher Tu_s values for lower blowing ratio (M=0.28)
- For higher blowing ratio, η decreases with increasing Tu_s but is not sensitive to higher turbulence values

M	Tu_s	Average Effectiveness
0.28	0	0.39
0.28	10%	0.53
0.28	15%	0.51
1	0	0.69
1	10%	0.64
1	15%	0.65

I-B-Effect of Slot Turbulence

- Secondary shear stress contours does not support presence of stationary streamwise vortices in the presence of higher Tu_s
- Turbulence at slot exit prevents early formation of K-H structures and reduction of streamwise-oriented structures. Leads to better film coverage on the surface

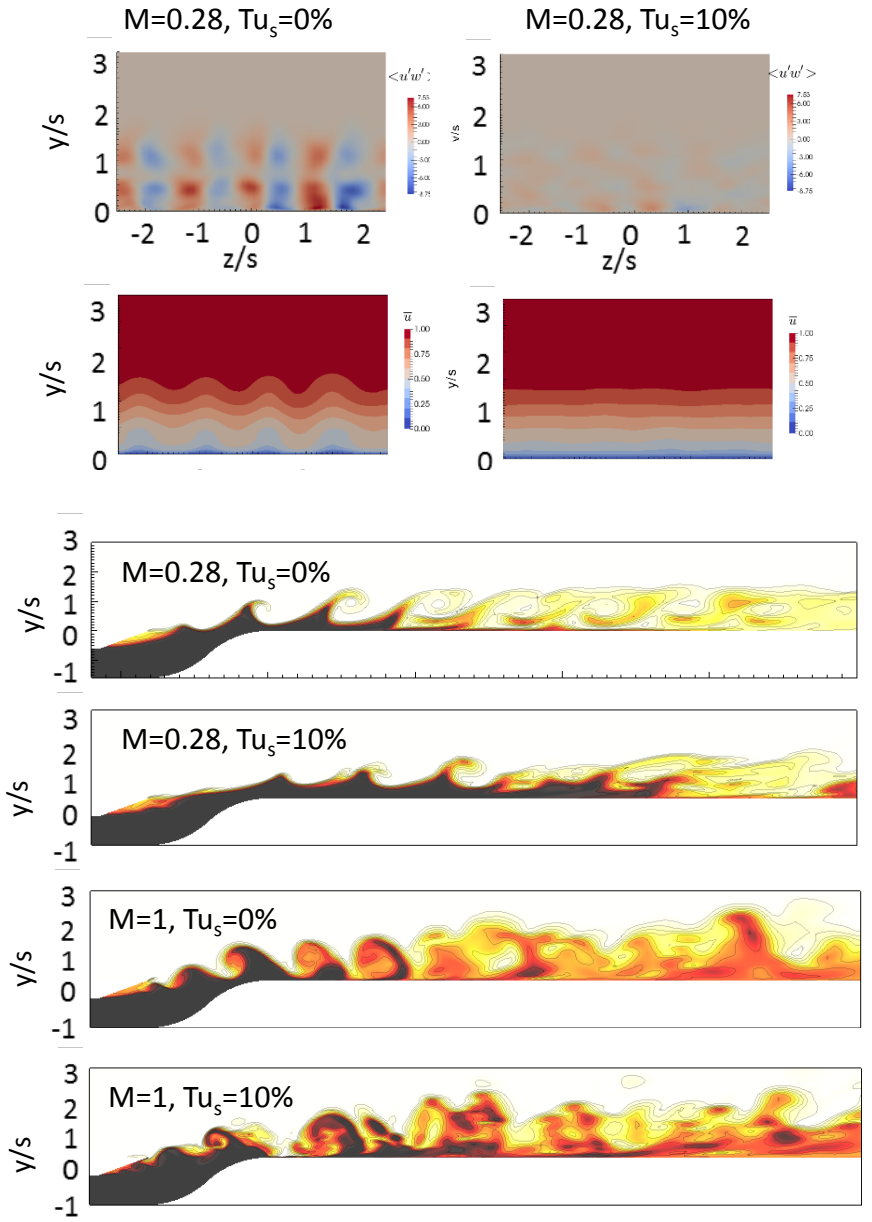

I-A-Turbulence effect on film cooling

- Slot cooling correlations in the literature do not account for inflow turbulence
- Data typically does not correlate well in the near-slot region

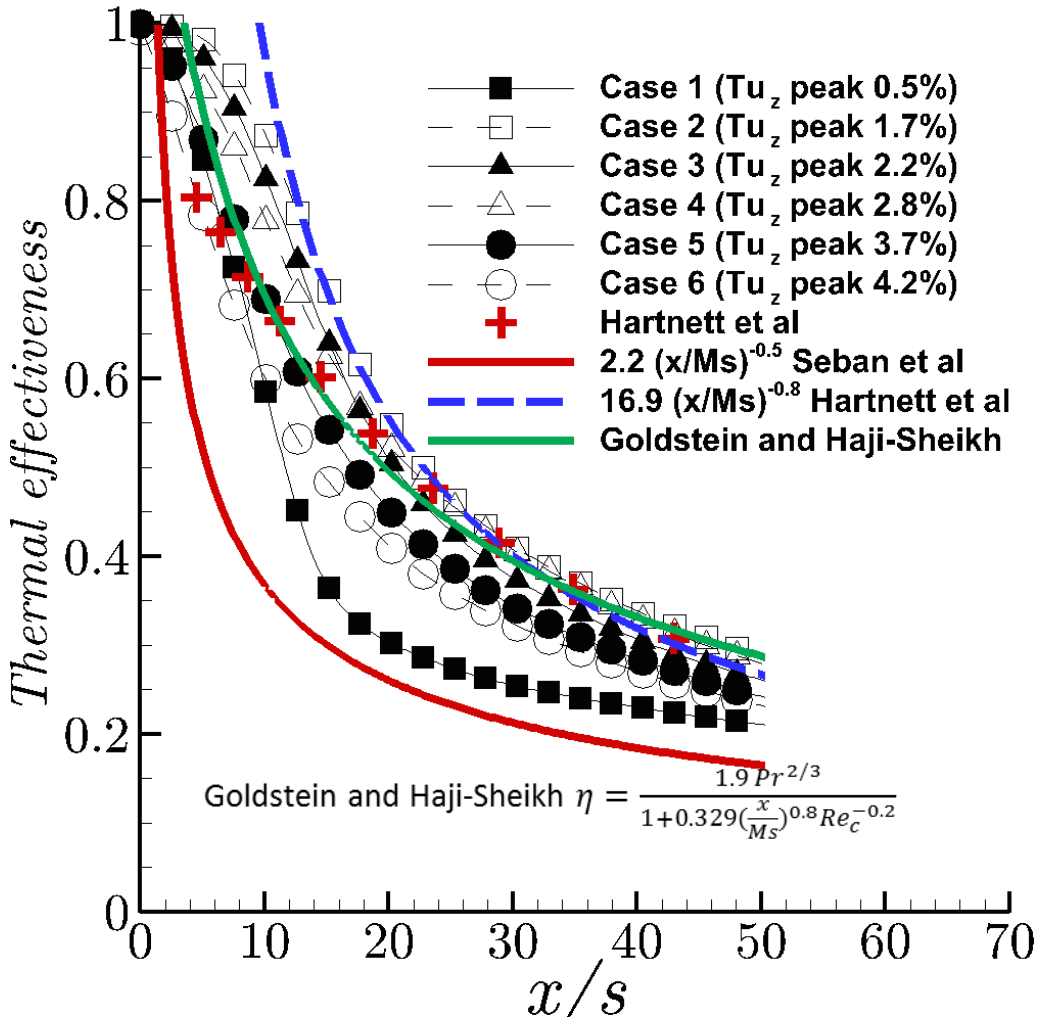

I-A-Slot Cooling Correlations

Goals:

Develop correlation which accounts for:

- Blowing Ratio
- Freestream Turbulence
- Freestream Acceleration

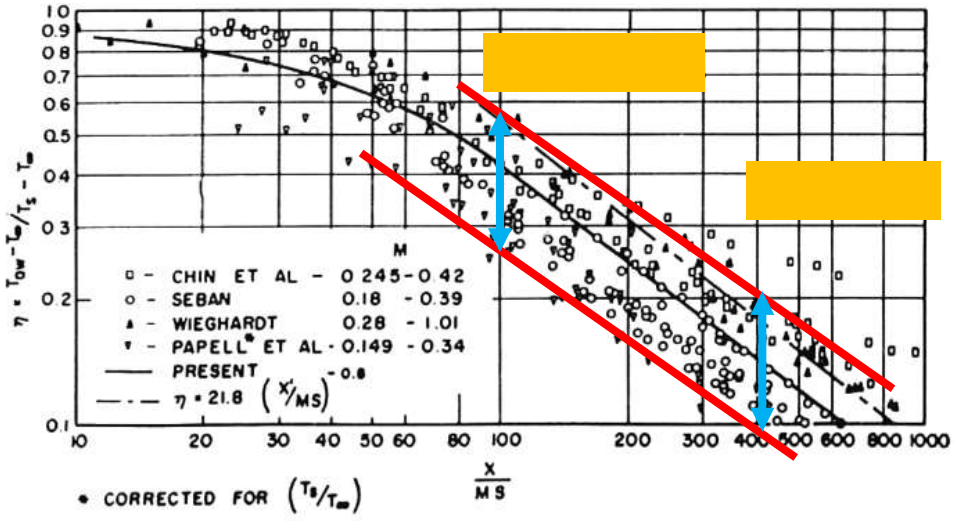

Available correlations

- Mostly valid for large x/Ms values (x/Ms>40)
- Do **NOT** account for **Freestream turbulence**
- Do **NOT** account for **Slot geometry (e.g. Injection angle)**
- Do **NOT** account for **Acceleration**

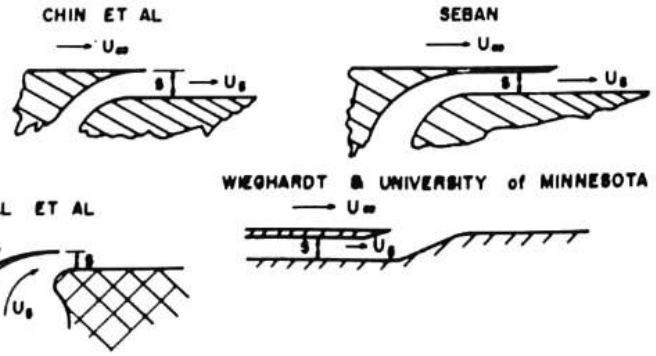

Well-known available correlations for slot cooling

- Hartnett $\eta = 16.9\,(\frac{x}{Ms})^{-0.8}\ \frac{x}{Ms} > 40$
- Spalding $\eta = \begin{cases} 1 & X < 7 \\ 7/X & X \geq 7 \end{cases}$ where $X = 0.91\left(\frac{x}{Ms}\right)^{0.8} Re_c^{-0.2} + 1.41\left\{\left|1 - \frac{1}{M}\right|\frac{x}{s}\right\}^{0.5}$
- Seban (M<0.6) $\eta = 25\,(\frac{x}{M^{1.5}s})^{-0.8}$ (tangential injection)
- Seban $\eta = 2.2\,(\frac{x}{Ms})^{-0.5}\ \frac{x}{Ms} > 40$ (normal injection)
- Goldstein and Haji-Sheikh $\eta = \frac{1.9\,Pr^{2/3}}{1+0.329(\frac{x}{Ms})^{0.8} Re_c^{-0.2}}$

$\eta = A\,(x/M^a s)^B$ *where A & B are fns of Tu*

I-C-Slot cooling with Acceleration

Goals:

Validate numerical predictions
Study flow physics
Study the effect of upstream turbulence

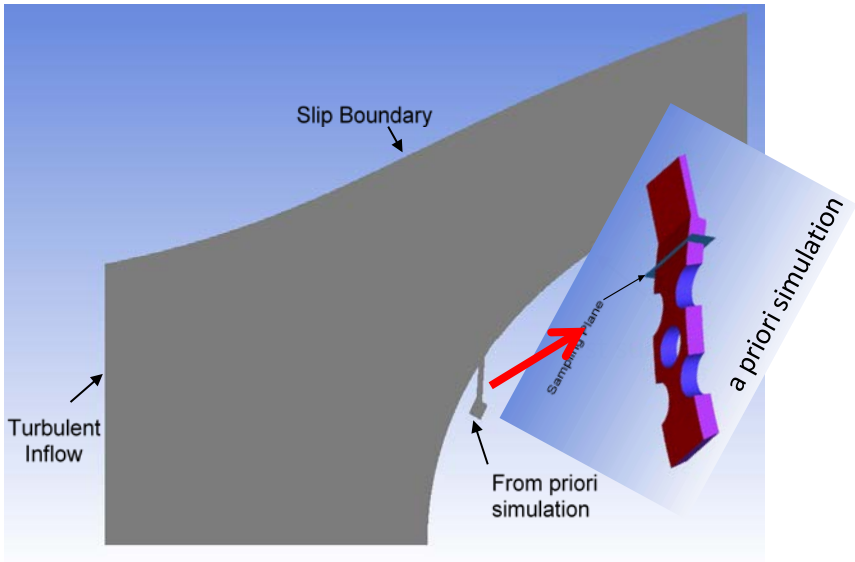

Flow Characteristics

Various turbulence conditions (0.7%, 3.5%, 7.8%, 13.7%)
Blowing Ratio M=0.78
Reynolds Number 250,000
Non uniform and turbulent flow at slot
(from a priori simulation)

Numerical Simulation

LES (dynamics SGS model)
16 Million grid points
Adiabatic / Heated test surface

***Busche, M L, and F E Ames. 2014. “Slot Film Cooling Measurements on an Accelerating Test Surface Subjected a Range of Turbulence Conditions.” In *Proceedings of ASME Turbo Expo 2014*,

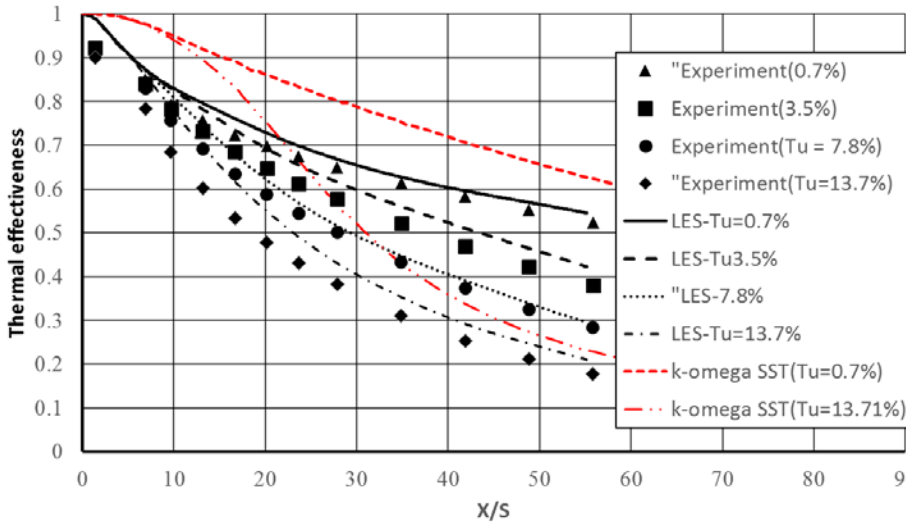

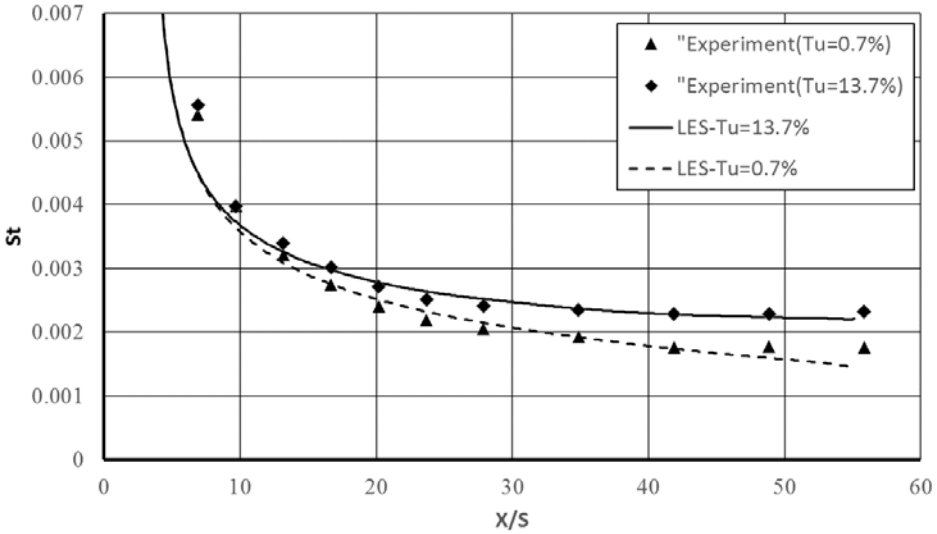

I-C-Flow Physics and Heat transfer

Flow Characteristics at slot

Average blowing ratio (M=0.78)
Non uniform turbulent flow in spanwise direction
Higher blowing ratio between pin fins
Higher Turbulence downstream of pin fins
Presence of elongated vortex tube (due to high acceleration)

Flow Characteristics at surface

Flow separation (bubble size of about one slot height)
Larger separation bubble at higher slot exit velocities
High Turbulence at the separation area (enclosed in the coolant jet)

Temperature Characteristics at Surface

Lower effectiveness downstream of pin fins where:
- blowing ratio is minimum
- turbulence is maximum

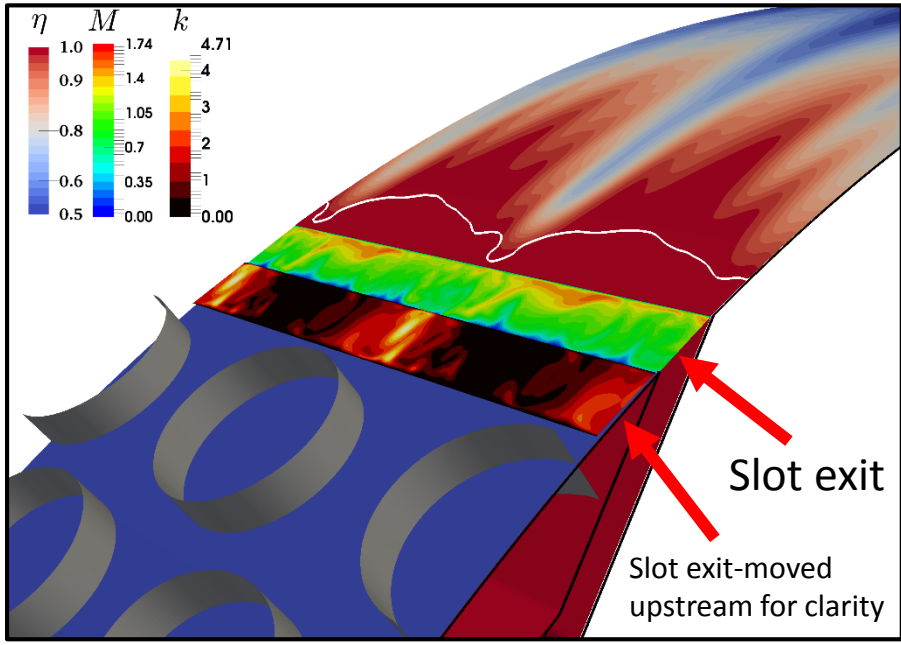

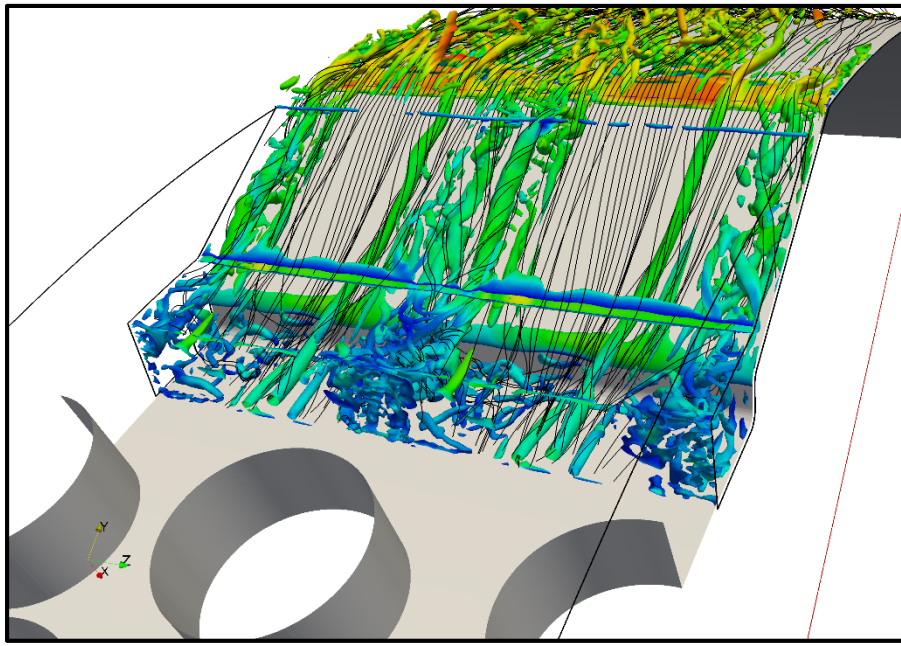

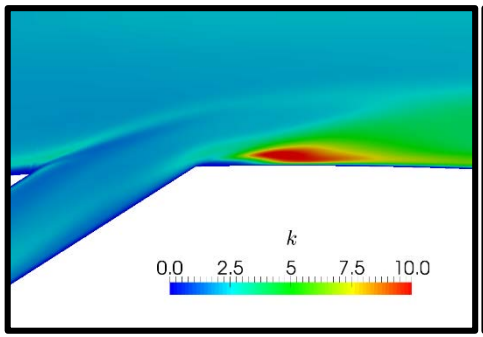

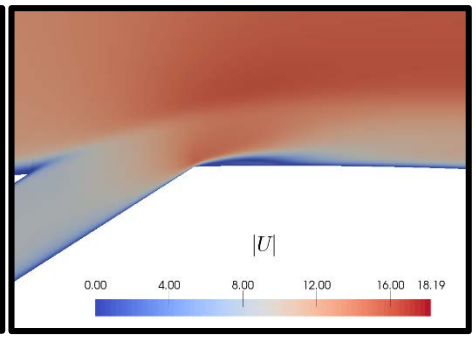

I-C-Effect of Turbulence

Flow field overview

- Turbulence generation in shear layer
- Turbulence generation in separation bubble (a, b)
- Amplification of peak turbulence at BL by freestream turbulence (a)
- Higher Reynolds shear stress (i.e. turbulence generation) near the wall for higher freestream turbulence conditions (b)

Temperature field overview

- Higher thermal diffusivity in BL for higher turbulence conditions (i.e. flatter thermal boundary layer) (d)

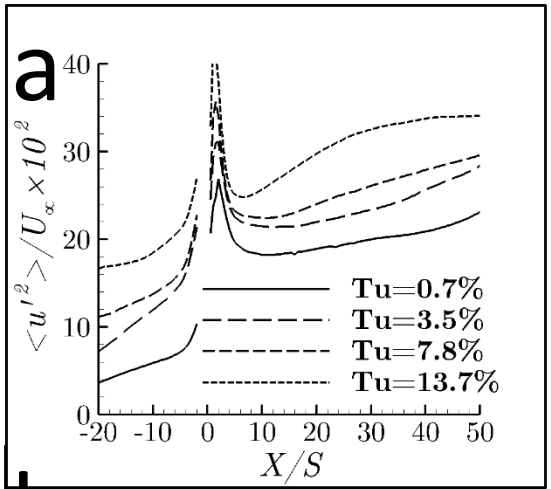

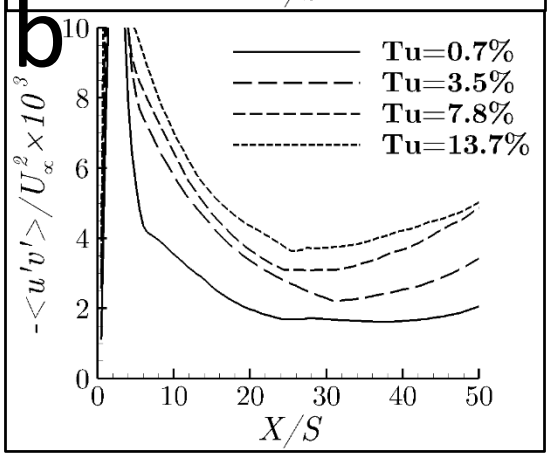

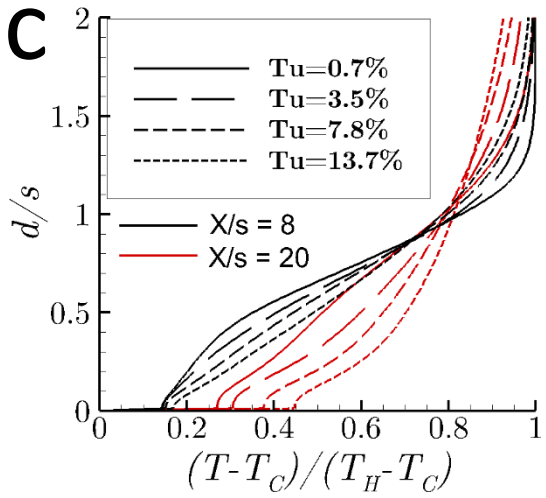

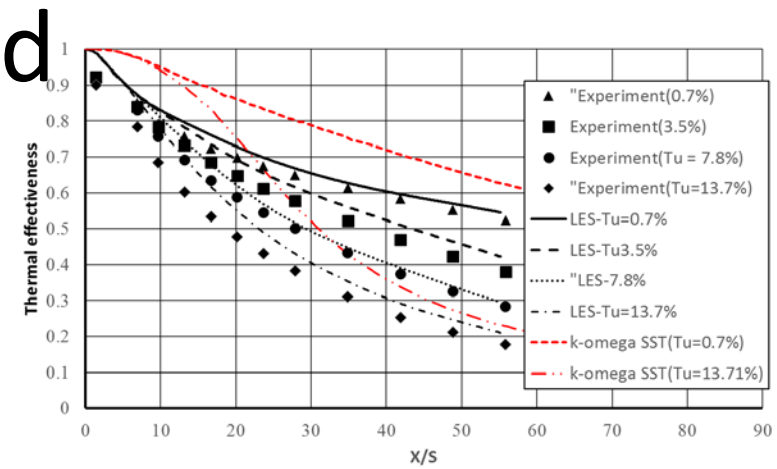

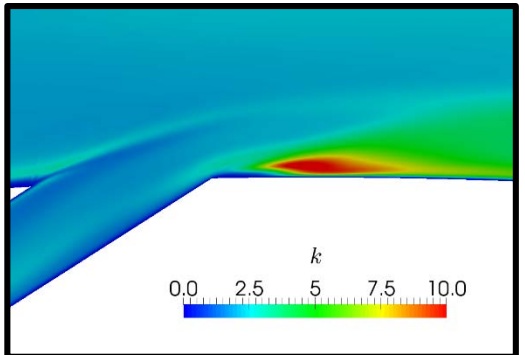

I-C-Slot Cooling Correlations

- Step 1: finding scaling parameter (Busche and Ames 2014)*

-Traditional scaling $\frac{x}{Ms}$

-Does not scale well specially for lower turbulence conditions

Hartnett's Correlation:

$$\eta = 16.9\,(\tfrac{x}{Ms})^{-0.8}\,\tfrac{x}{Ms} > 40$$

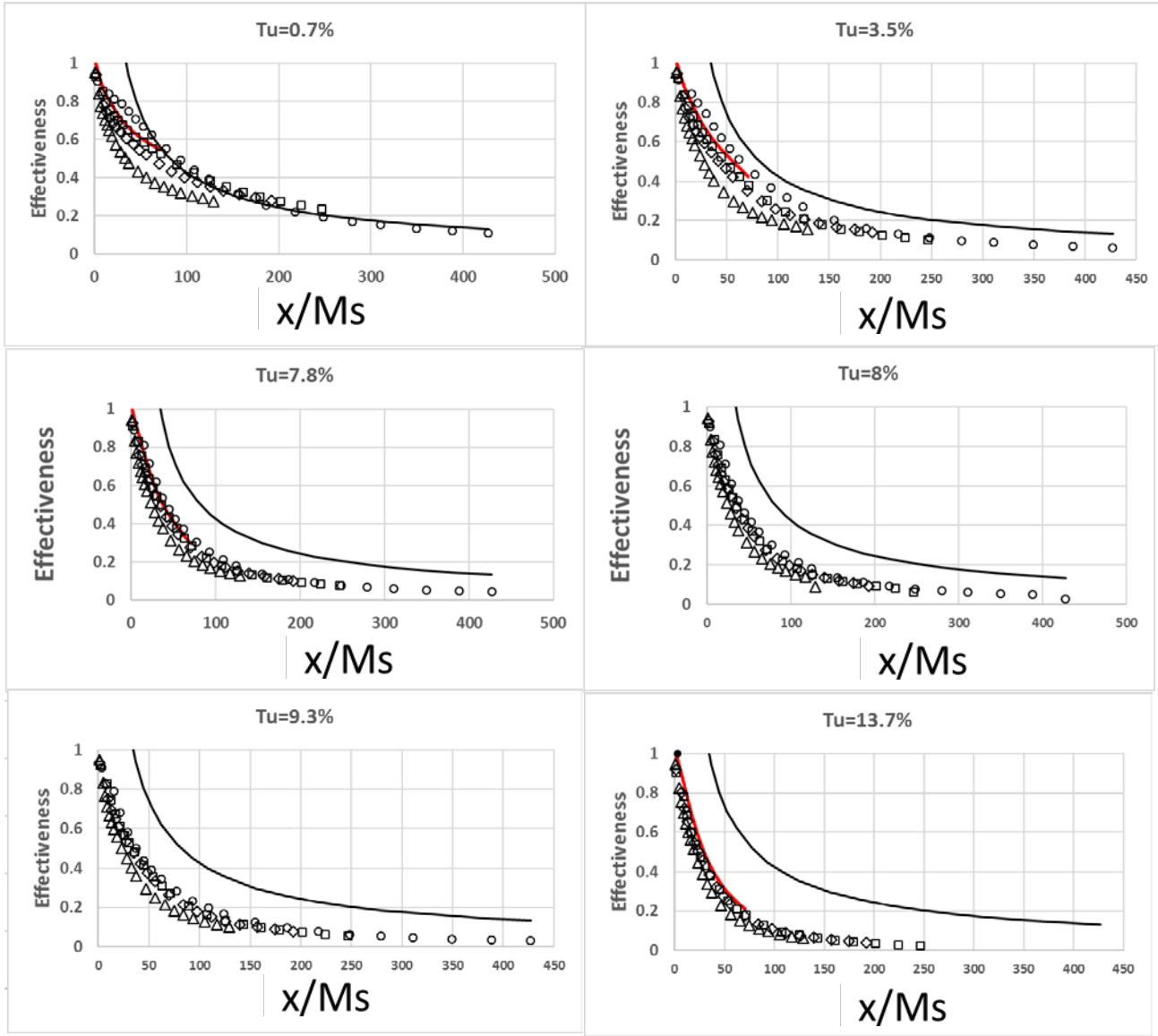

*Busche, M L, and F E Ames. 2014. "Slot Film Cooling Measurements on an Accelerating Test Surface Subjected a Range of Turbulence Conditions." In *Proceedings of ASME Turbo Expo 2014*,

I-C-Slot Cooling Correlations

- Step 1: finding scaling parameter (Busche and Ames 2014)*

  - Our scaling
  - Significant improvement in scaling in most range of turbulence conditions

Hartnett's Correlation:

$$\eta = 16.9\,(\frac{x}{Ms})^{-0.8}\,\frac{x}{Ms} > 40$$

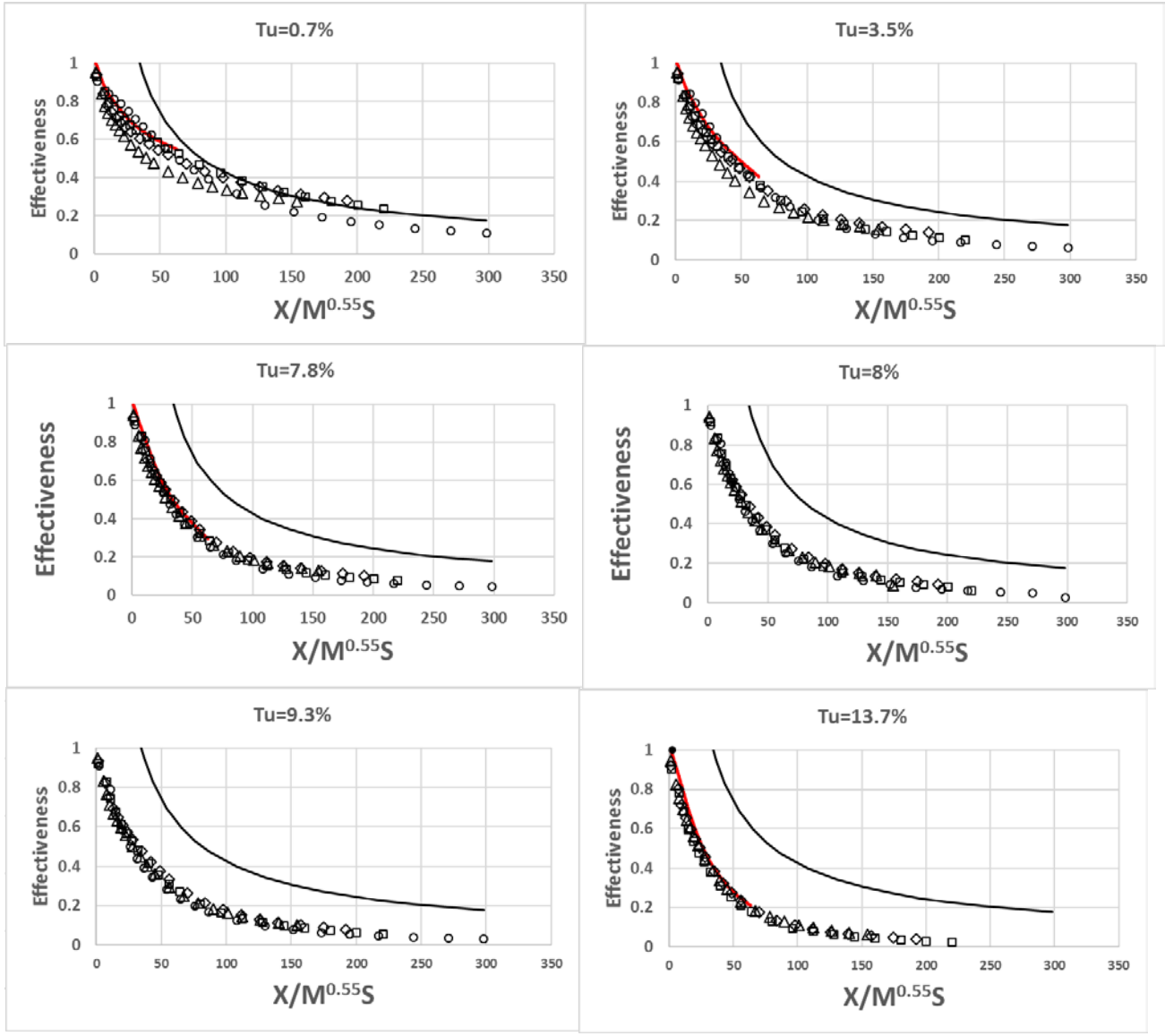

*Busche, M L, and F E Ames. 2014. "Slot Film Cooling Measurements on an Accelerating Test Surface Subjected a Range of Turbulence Conditions." In *Proceedings of ASME Turbo Expo 2014*,

I-C-Slot Cooling Correlations

- Step 2: finding the correlation (UND data)
  - Correlation: $\eta = A\left(\frac{x}{M^{0.55}S}\right)^n$
  - All data except the low turbulence data is used for the correlation development

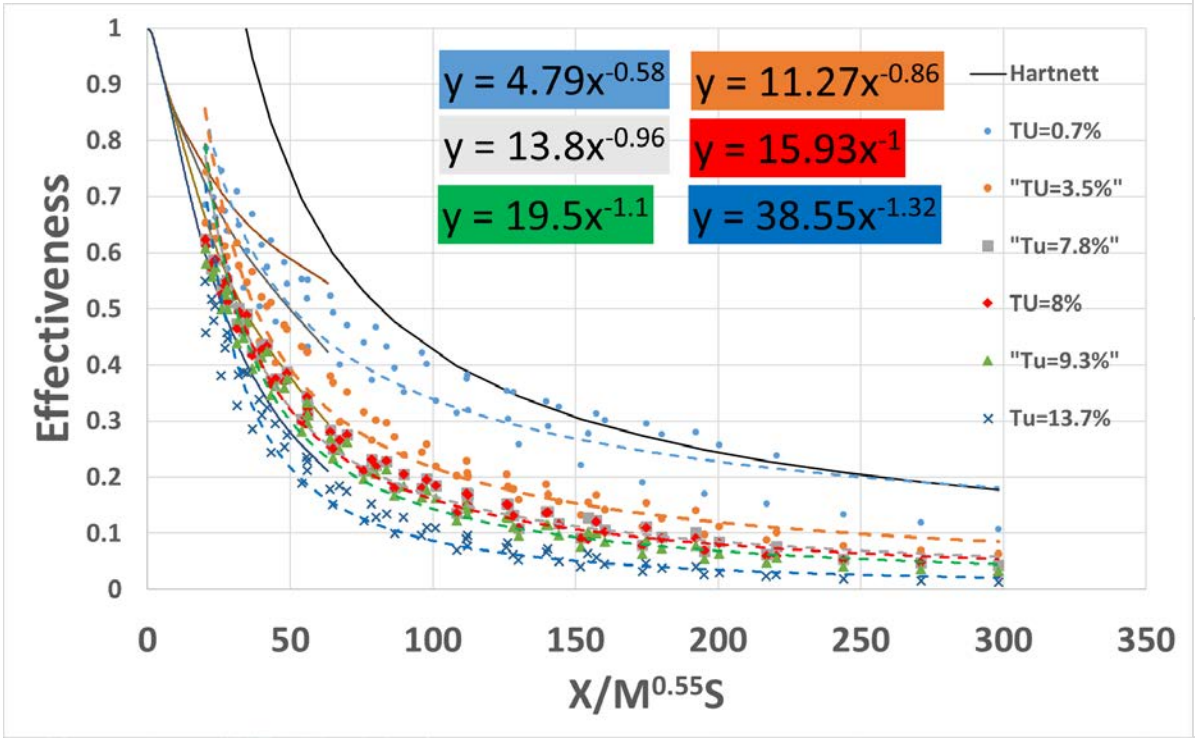

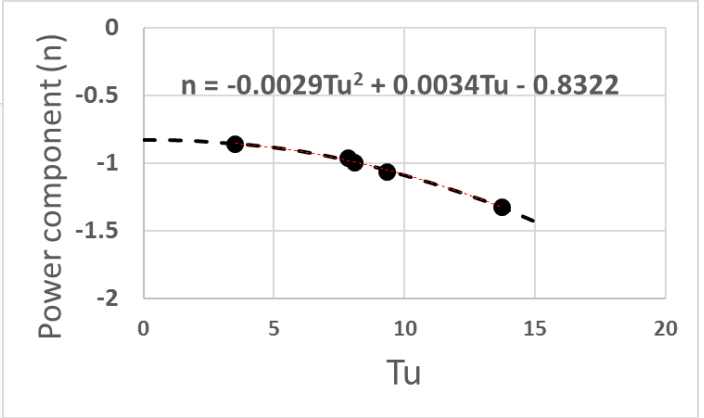

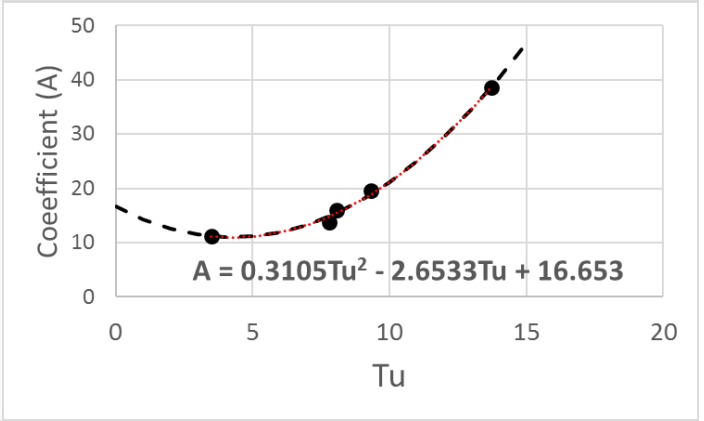

I-C-Slot Cooling Correlations

- Step 3: Evaluating the Correlation accuracy with other data

data by lebedev 1991*

- Clear improvement compared to Hartnett's correlation
- Suggested Correlation perform better for higher turbulence cases

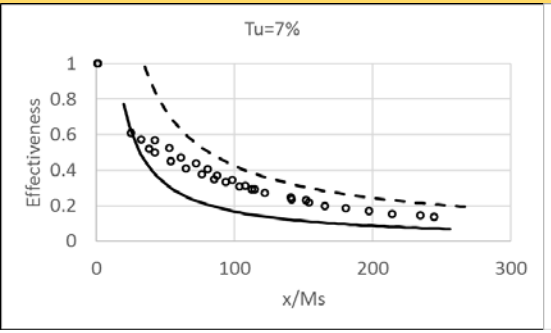

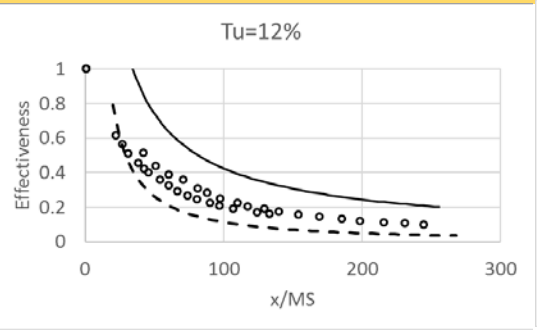

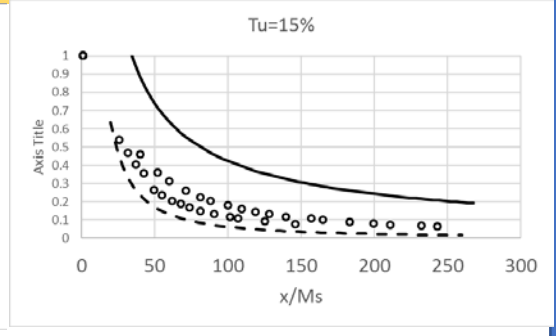

Solid: Hartnett Correlation

Dashed: This work

Symbols: Experimental data

data by Simons 1986**

- Very good prediction of the effectiveness except for the lowest turbulence

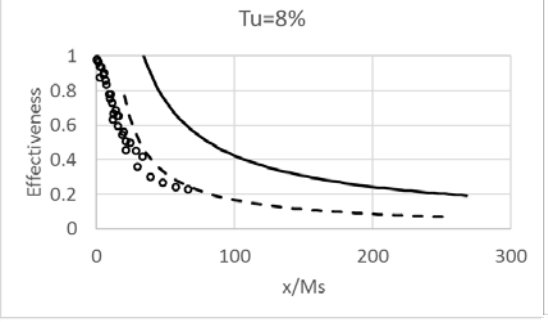

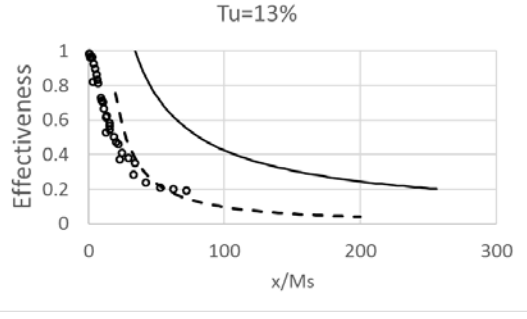

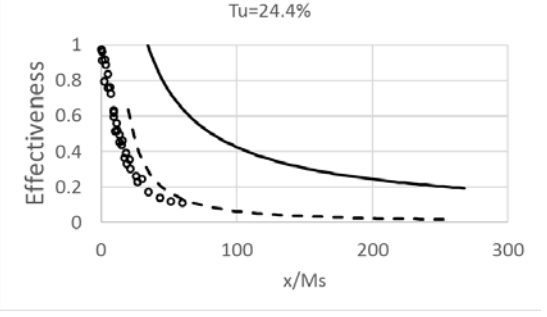

data by Bunker (Tu=4%)***

- Very good prediction of the effectiveness for most blowing ratios

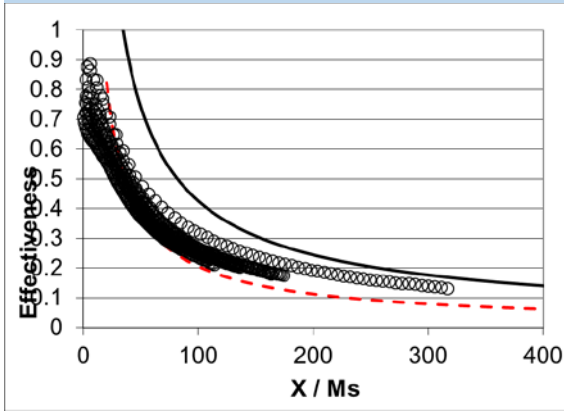

*V.P. Lebedev, V. V. Lemanov, S.Y. Misyura, V.I. Terekhov, Effects from turbulence intensity on slot protection performance, J. Appl. Mech. Tech. Phys. 32 (1991) 360–364. doi:10.1007/BF00852139.

**F. Simon F, Jet Model for Slot Film Cooling With Effect of Free-Stream and Coolant Turbulence, (1986).

***R.S. Bunker, A Study of Mesh-Fed Slot Film, J. Turbomach. 133 (2011) 011022,1-8. doi:10.1115/1.4000548.

Cascade Heat Transfer

- Case setup identical to Varty and Ames*
- Various turbulent conditions at inlet
- Various Reynolds number
- Unheated/Heated Endwall
- Incompressible Navier-Stokes
  - 2nd order scheme
- URANS (Gamma-Re Transition Model)
  - 1.8M-5M Grid points
- LES
  - 50M Grid points

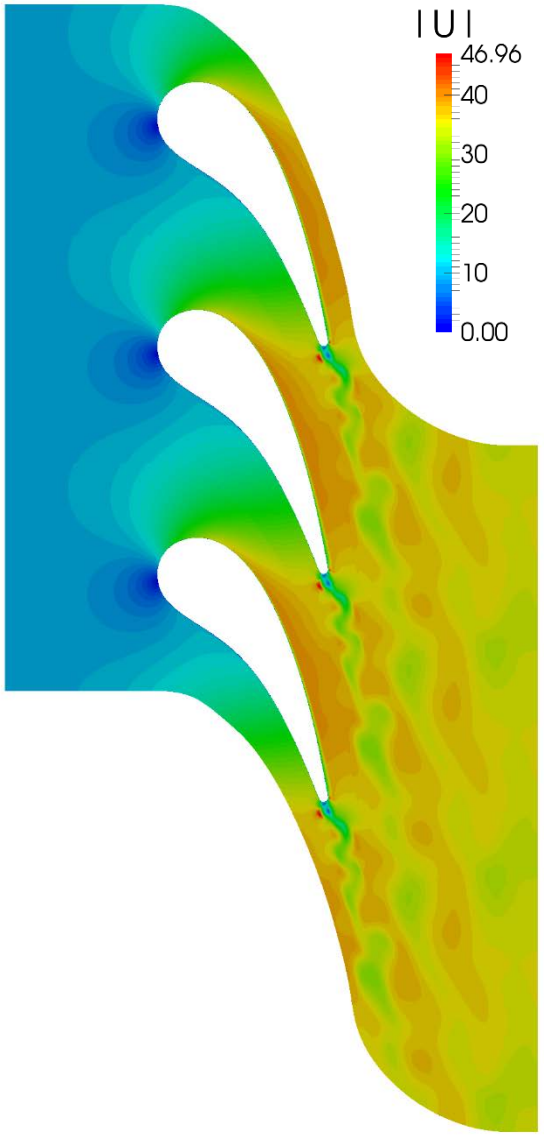

*Varty, Justin W, and Forrest E Ames. 2016. "Experimental Heat Transfer Distributions Over An Aft Loaded Vane With A Large Leading Edge At Very High Turbulence Levels." In *ASME 2016 International Mechanical Engineering Congress and Exposition IMECE2016*, Phoenix.

II-Internal cooling with pedestals and incremental coolant impingement

- Wall-resolved LES study
- Calculations are done for a range of Re and geometrical parameters
  - Validation (Ames & Dvorak, Busche et. al.)
  - HTC correlations

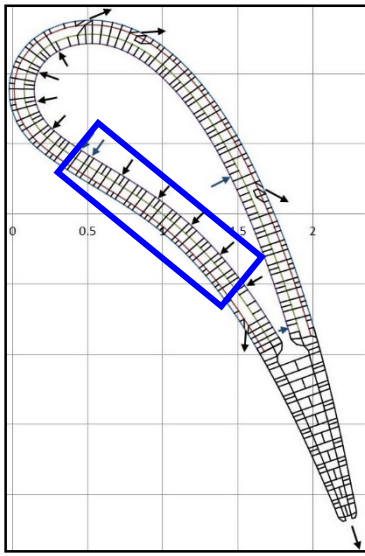

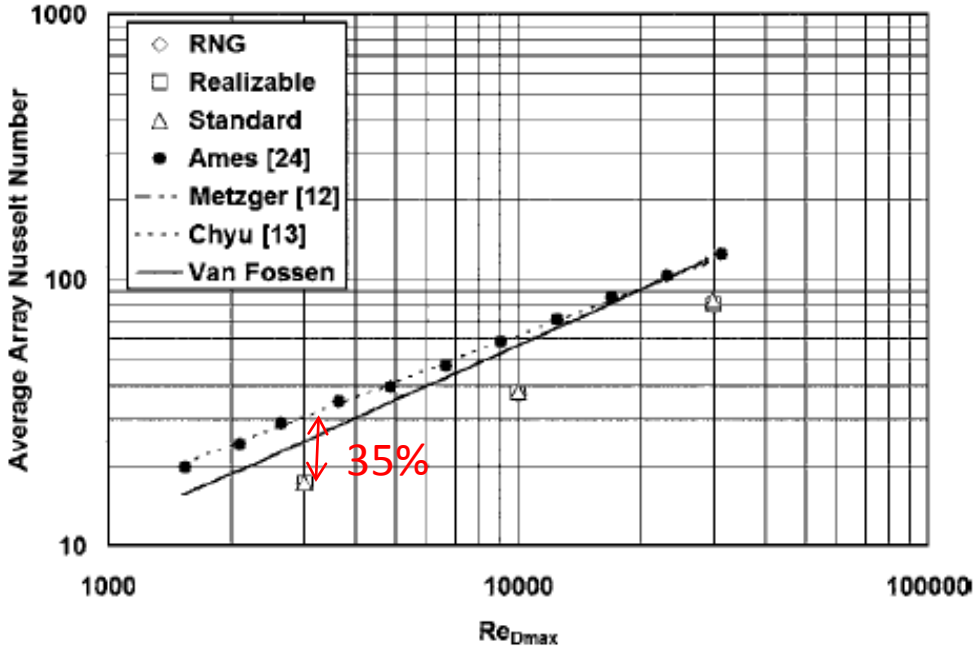

Comparing RANS w/ Data (Ames & Dvorak, 2006)

II-Computational Geometry

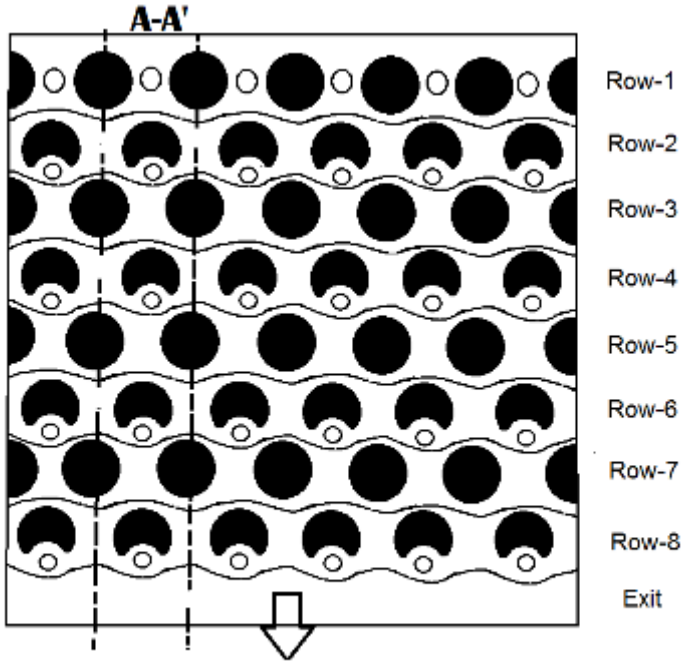

Multiple impingement rows

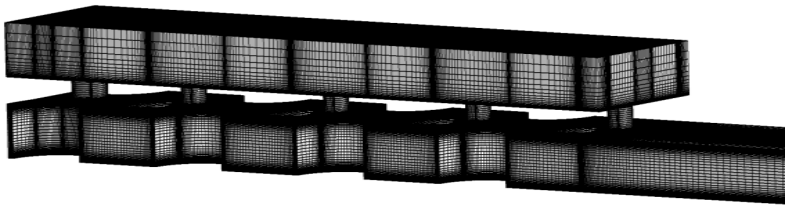

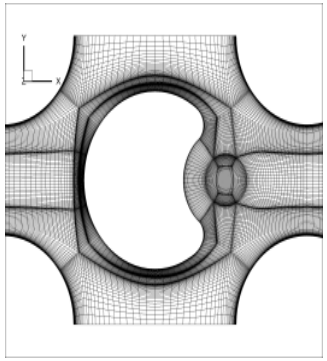

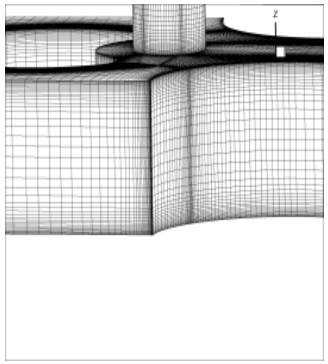

Meshing Detail s– Block structured mesh, Y+ <1
771 blocks- 4million

- In house CHEM3D code
- Fifth order WENO Scheme for convection;
- Second order CD scheme for diffusion
- Second order time integration
- Tested for scalability up to 1000 processors
- LES with D-S-L model

II-Thermal Eff. Predictions Agree Well with Data

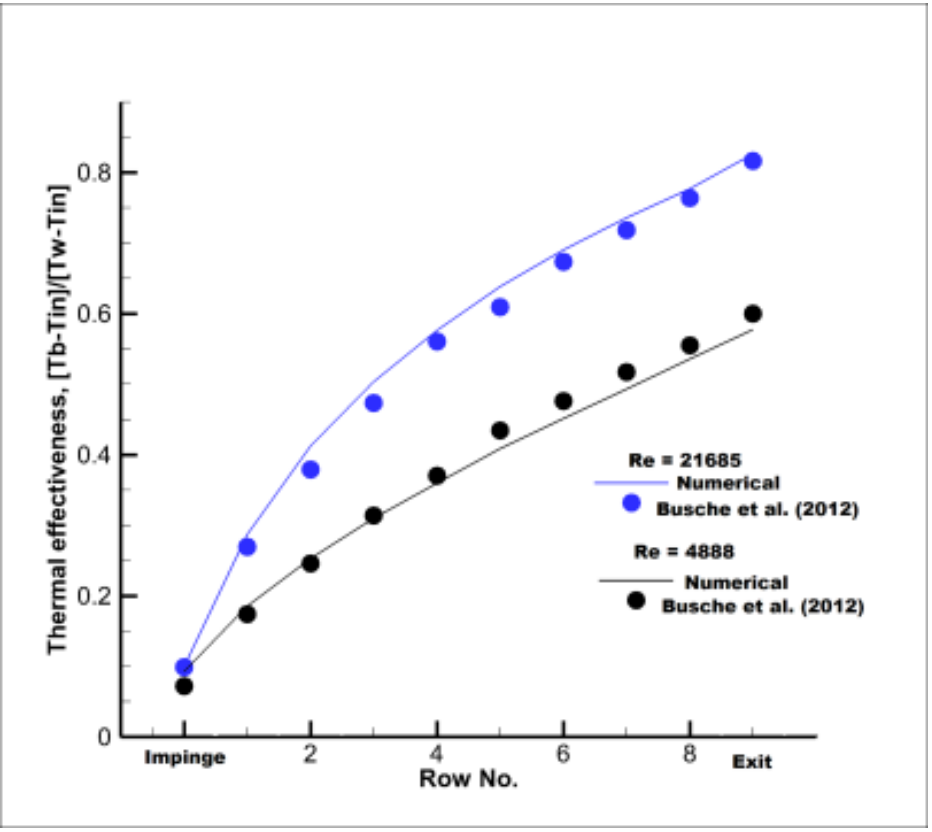

Baseline configuration

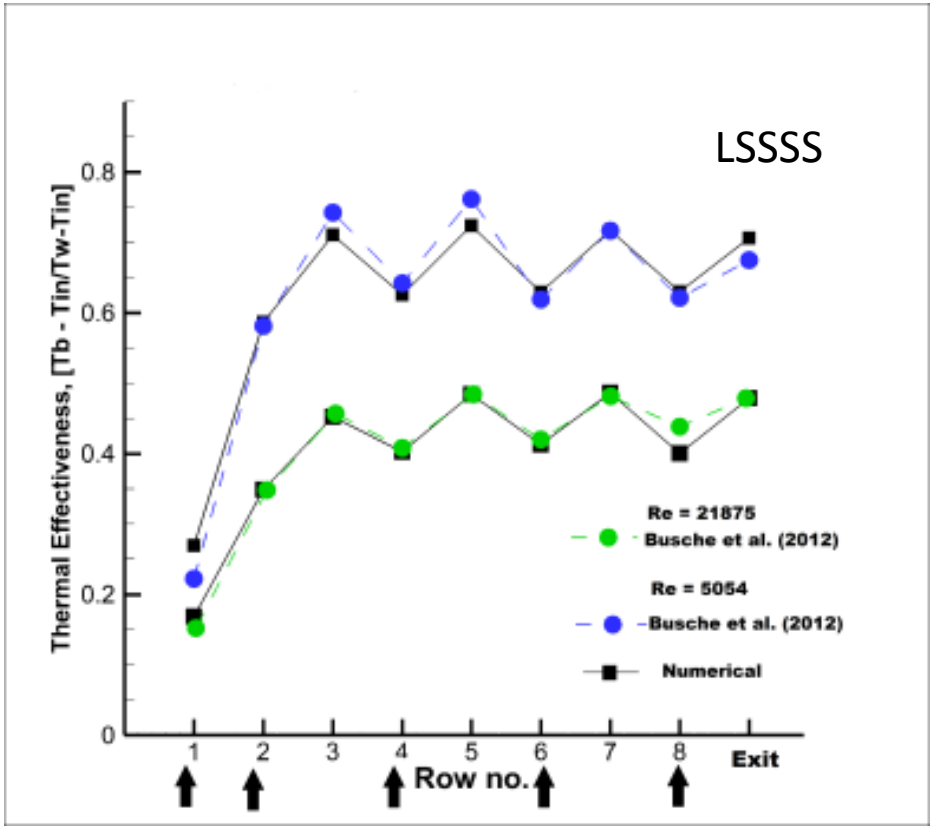

Incremental Impingement

Comparison with UND Data

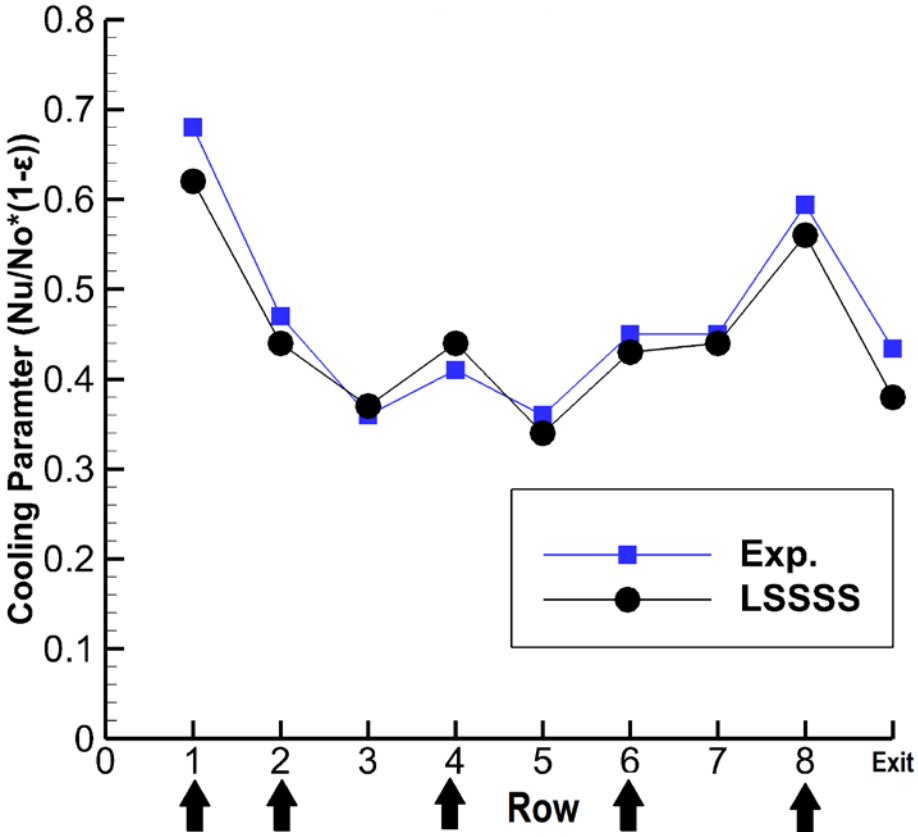

LSSSS (Re = 7,500)

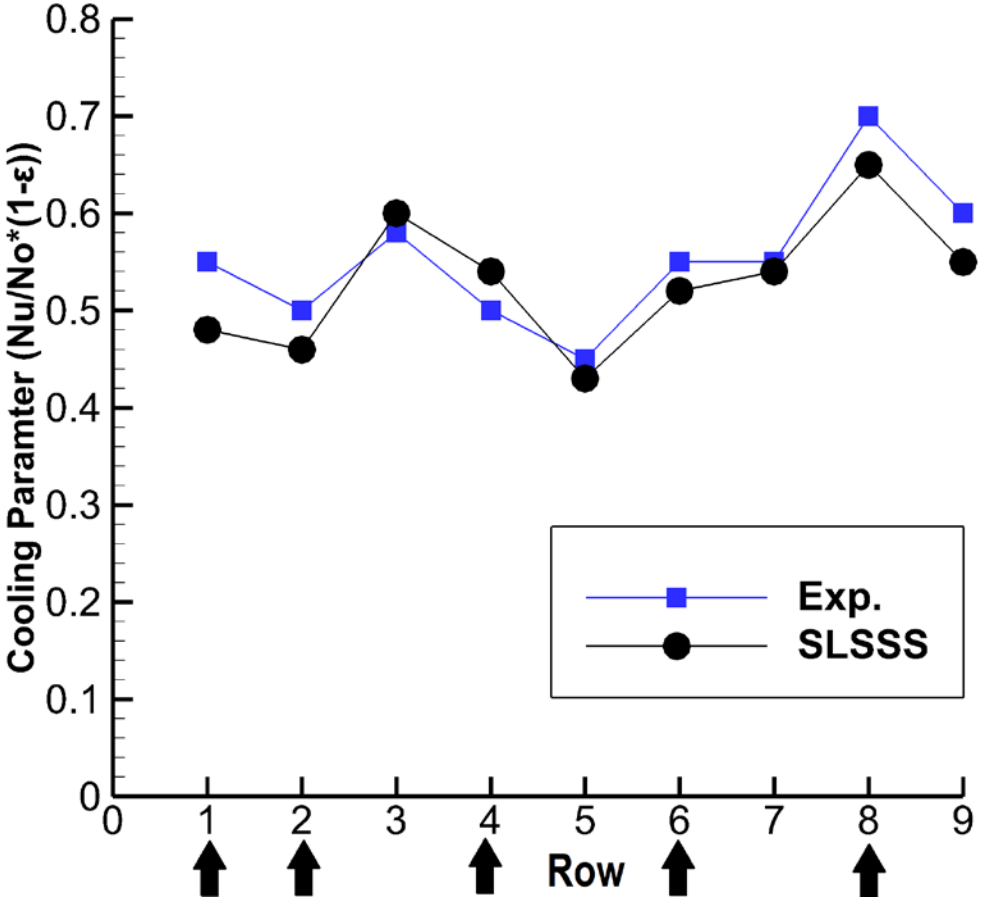

SLSSS (Re = 15,000)

II-Incremental Impingement Avoids Deflection by the Crossflow

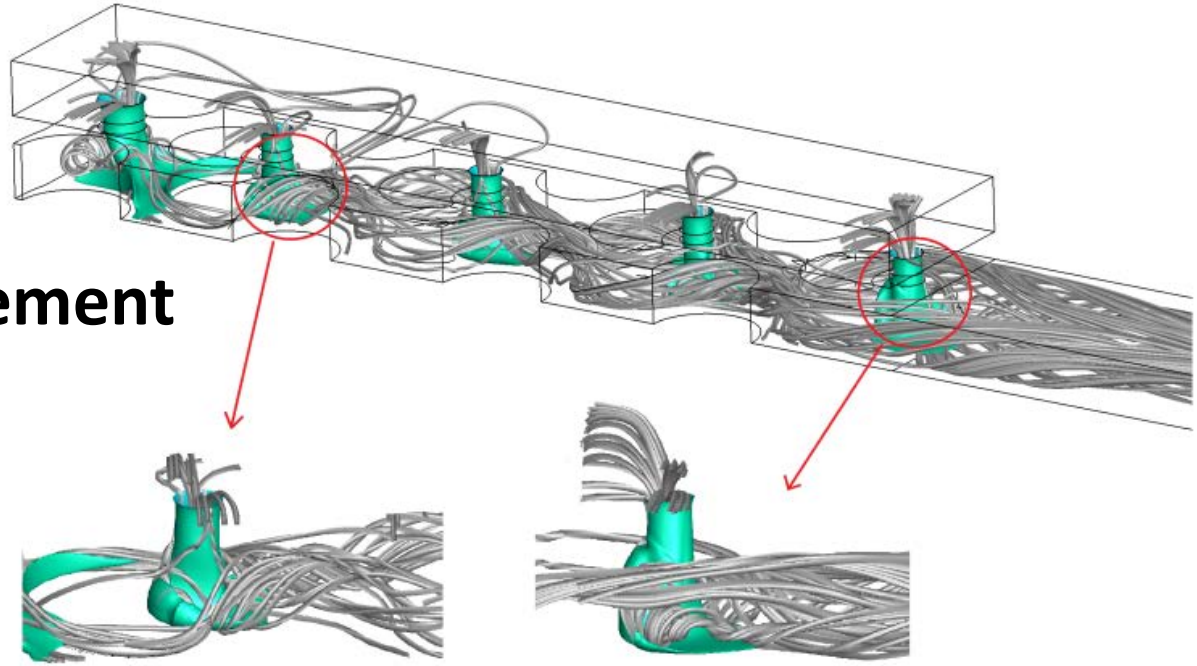

Incremental Impingement

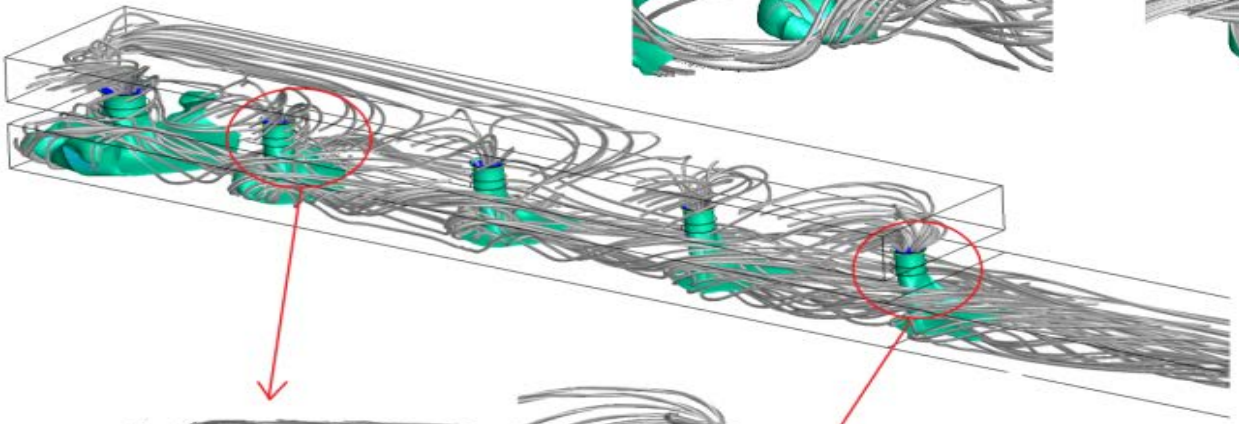

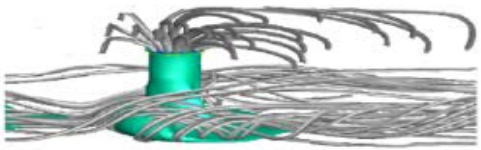

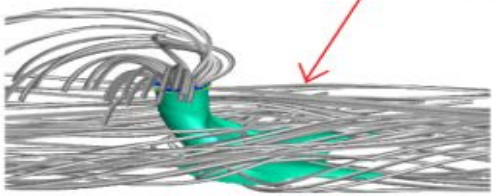

Impingement Only

II-Incremental Impingement Nu vs Baseline Cases

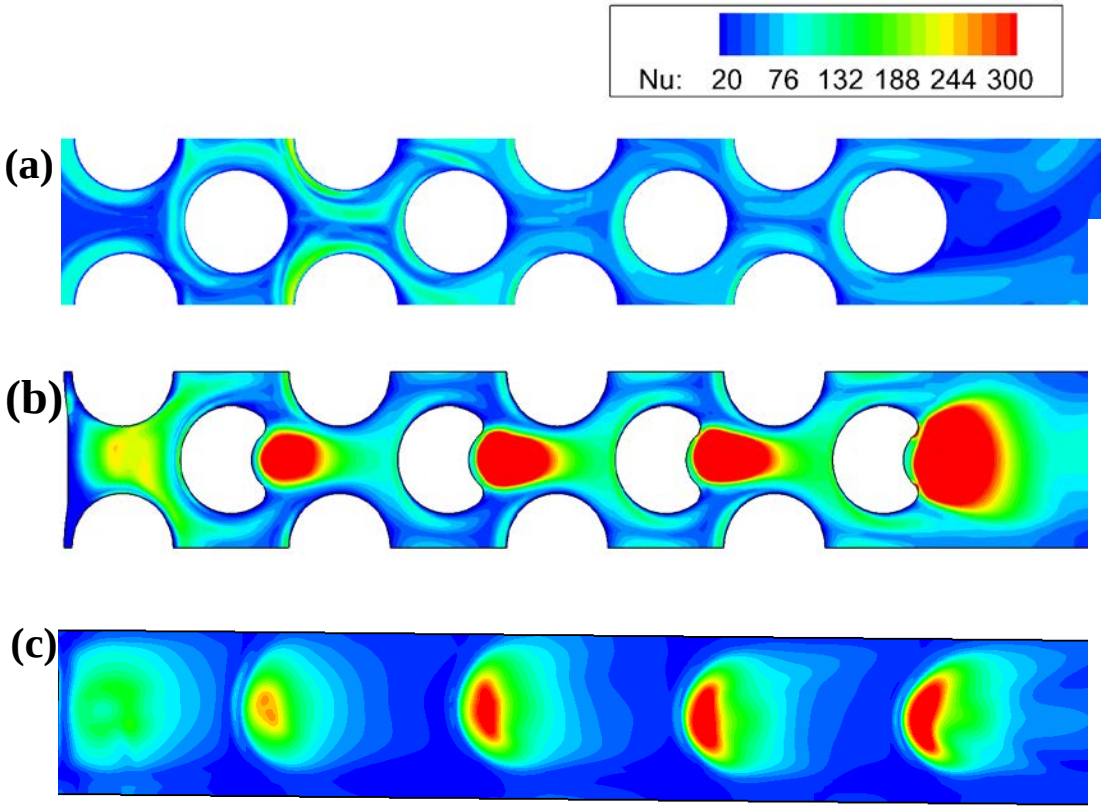

Nusselt number contour on end wall

a) Straight inlet b) Incremental impingement c) Impingement-no fins

LSSSS
Re=20,000

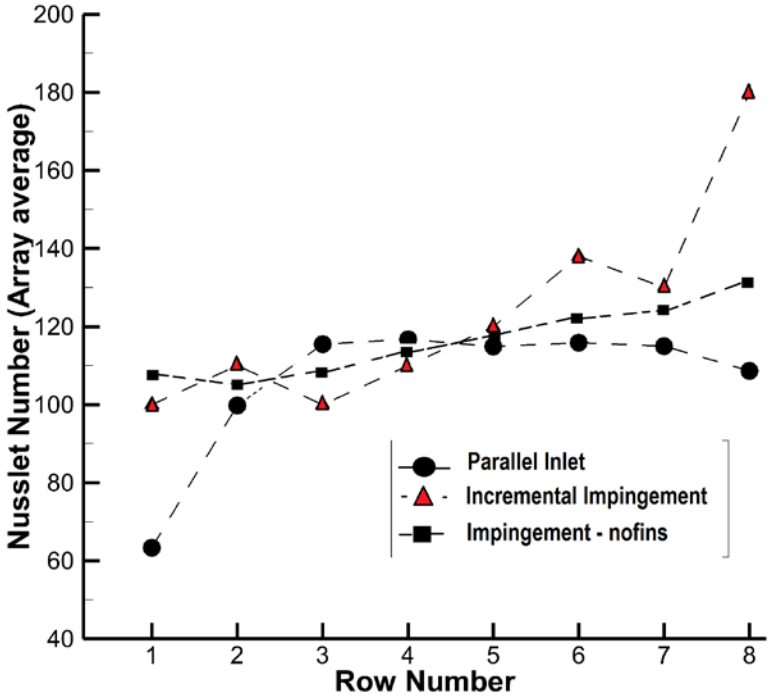

II-Jet-Flow Structures

Jet-2 – 2.862 ms-1
Jet-6 – 4.291ms-1
LSSSS configuration
Re = 7500

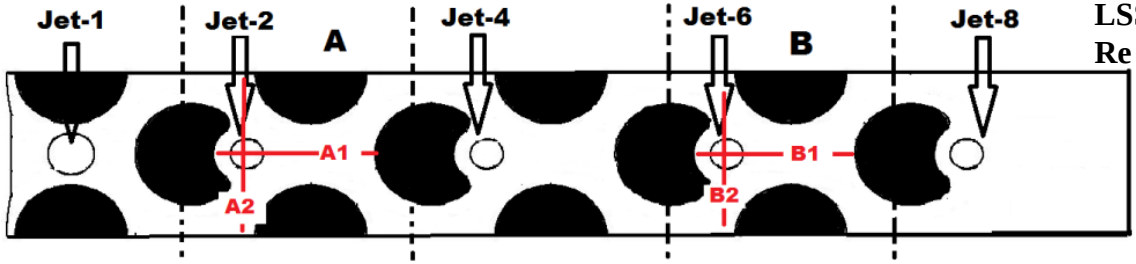

B1

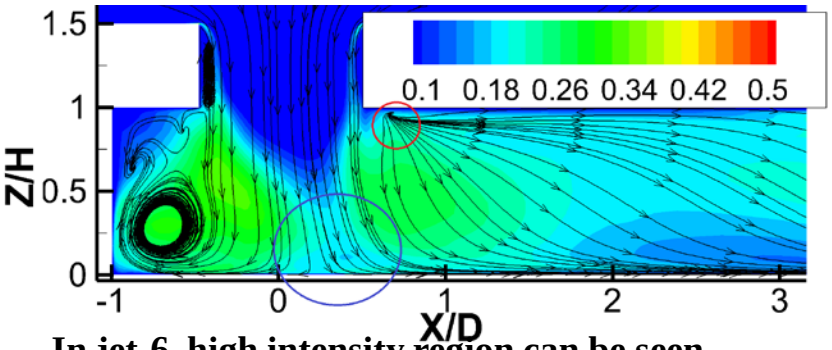

B2

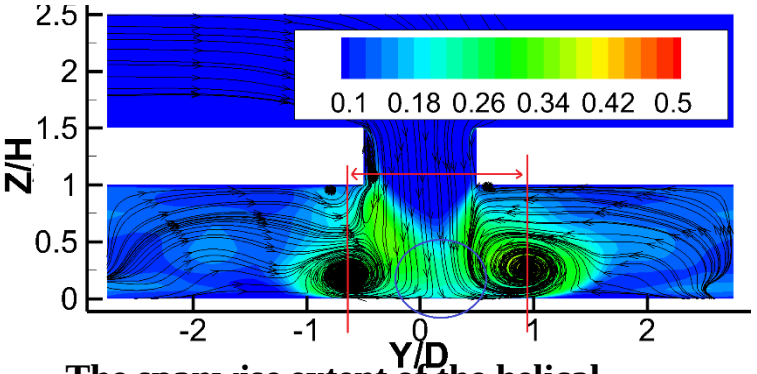

In jet-6, high intensity region can be seen near stagnation region (circled in blue)

The spanwise extent of the helical vortex is shown by red arrow.

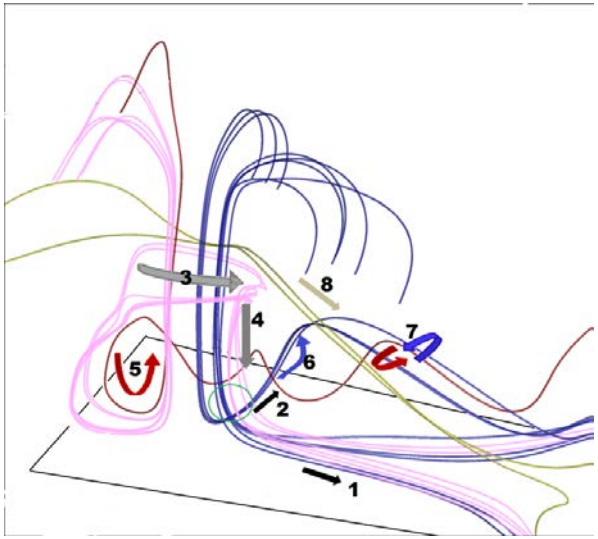

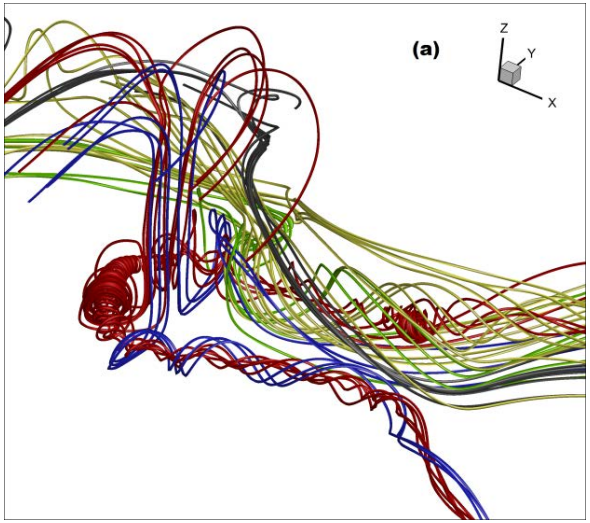

II-Hole Sizes & Distributions

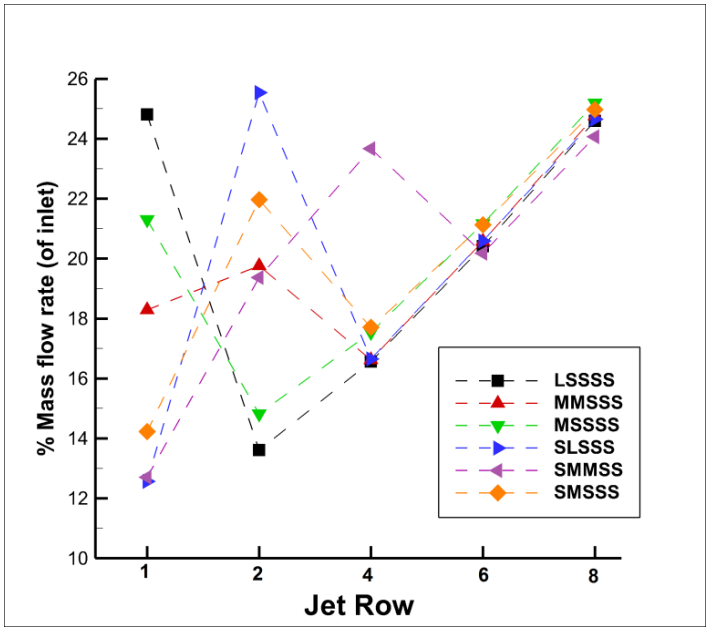

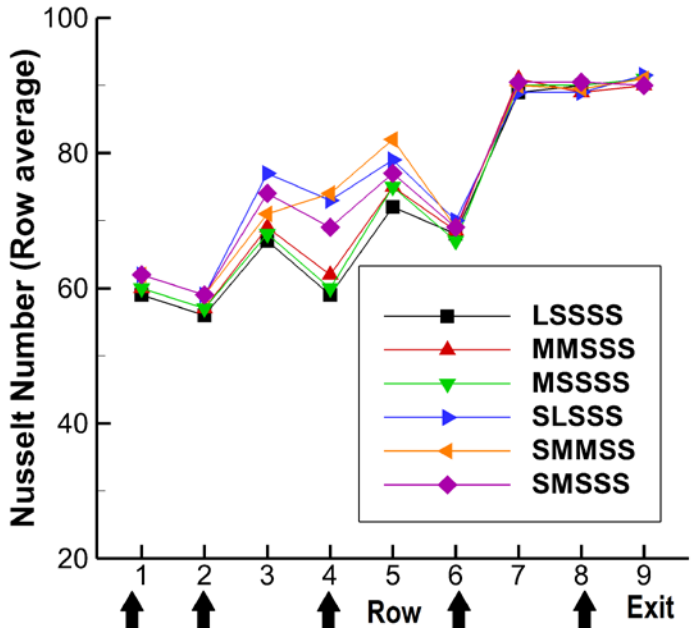

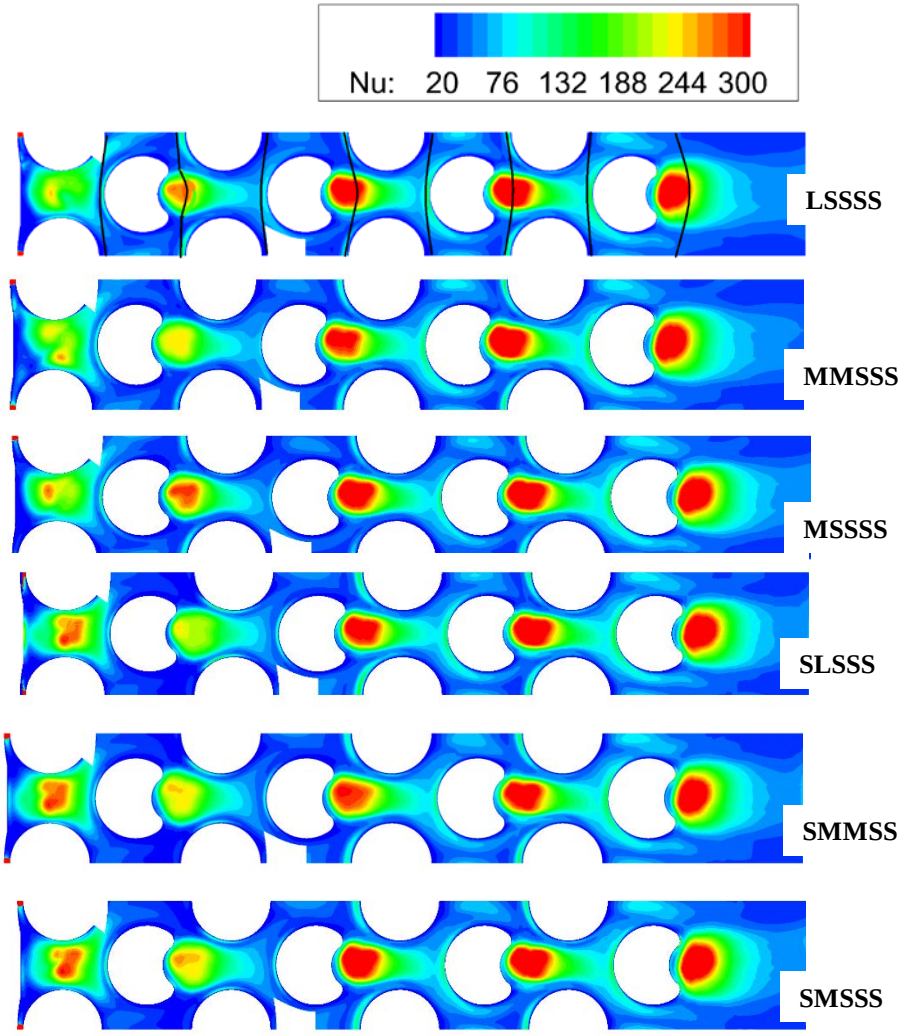

S/D = 1.625
X/D = 1.074
Re = 7,500

II-Correlations

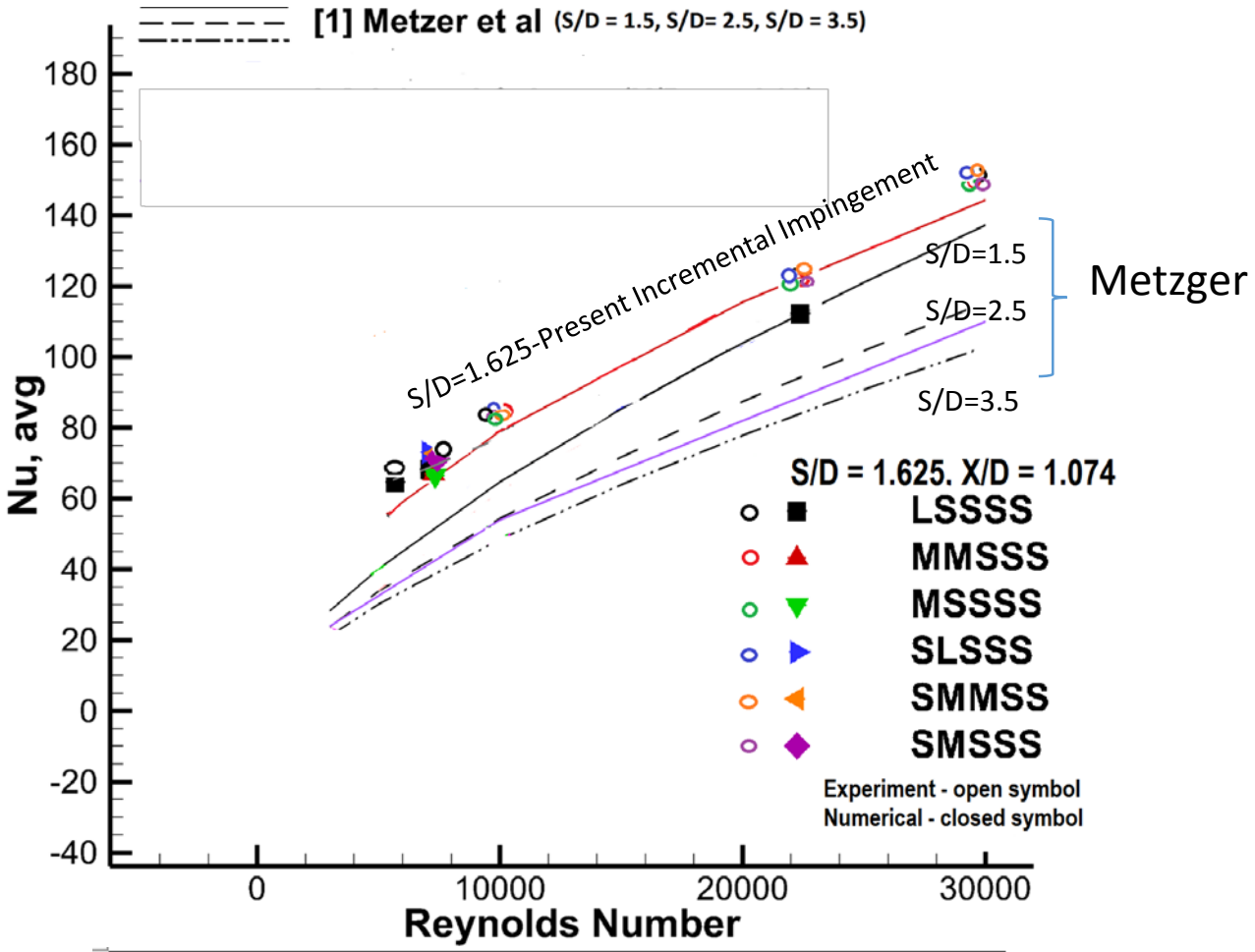

Sl. No.	Correlations	Authors
1.	$Nu = 0.135\ Re^{0.685}\ (X/D)^{-0.34}$	Metzer et al.
2.	$Nu = 0.32\ Re^{0.583}$	Chyu et al.
3.	$Nu = 0.508\ Re^{0.548}$	Jaiswal and Ames
4.	$Nu = 0.069\ Re^{0.728}$	Metzer and Haley
5.	$Nu = 0.153\ Re_{D'}^{0.685}$	VanFossen

PRESENTATION SUMMARY

- The present research project combines a four phase experimental and analytical program to advance the readiness of three internal cooling methods.
- External midspan heat transfer distributions and full suction surface heat transfer data have been acquired on the vane showing the impact of turbulence and secondary flows while preparations for film cooling measurements are ongoing.
- Twenty six configurations of variable hole size incremental impingement have been tested providing a highly extended database for computational grounding of predictive methods. Trailing edge cooling measurements will follow shortly
- Internal heat transfer predictions show excellent promise in matching experimental data while helping to clarify the physics of the cooling method.
- External film cooling and heat transfer predictions have been challenging and wall resolved LES has been applied to cope with the complex physics of the film cooling and external heat transfer.
- The final vane cooling configuration will be selected shortly for warm cascade testing in order to advance the technology readiness of the internal cooling methods.